

Biomass Storage in Anoxic Marine Basins: Initial estimates of geochemical impacts and CO₂ sequestration capacity

Morgan Reed Raven¹, Molly Crotteau¹, Natalya Evans², Zephyr C Girard², Aaron Martinez², Izzy S Young², and David L Valentine³

¹University of California, Santa Barbara

²University of California Santa Barbara

³UC Santa Barbara

April 29, 2023

Abstract

In combination with dramatic and immediate CO₂ emissions reductions, net-negative atmospheric CO₂ removal (CDR) is necessary to maintain average global temperature increases below 2.0 °C. Many proposed CDR pathways involve the placement of vast quantities of organic carbon (biomass) on the seafloor in some form, but little is known about their potential biogeochemical impacts, especially at scales relevant for global climate. Here, we evaluate the potential impacts and durability of organic carbon storage specifically within deep anoxic basins, where organic matter is remineralized through anaerobic processes that may enhance its storage efficiency. We present simple biogeochemical and mixing models to quantify the scale of potential impacts of large-scale organic matter addition to the abyssal seafloor in the Black Sea, Cariaco Basin, and the hypersaline Orca Basin. These calculations reveal that the Black Sea in particular may have the potential to accept biomass storage at climatically-relevant scales with moderate changes to the geochemical state of abyssal water and limited communication of that impact to surface water. Many key unknowns remain, including the partitioning of breakdown among sulfate-reducing and methanogenic metabolisms and the fate of methane in the environment, which can be monitored in part via changes in alkalinity, DIC, and pH. Given the urgency of responsible CDR development and the potential for anoxic basins to reduce ecological risks to animal communities, efforts to address knowledge gaps related to microbial kinetics, benthic processes, and physical mixing in these systems are critically needed.

Hosted file

961817_0_art_file_10923911_rt11kx.docx available at <https://authorea.com/users/560136/articles/640305-biomass-storage-in-anoxic-marine-basins-initial-estimates-of-geochemical-impacts-and-co2-sequestration-capacity>

1 **Biomass Storage in Anoxic Marine Basins: Initial estimates of geochemical impacts and CO₂**
2 **sequestration capacity**

3
4 Raven M.R.,^{1*} Crotteau M.A.,¹ Evans N.,¹ Girard Z.C.,¹ Martinez A.M.,¹
5 Young I.,¹ Valentine D.L.¹
6

7 ¹ Dept of Earth Science, University of California Santa Barbara, Santa Barbara CA 93106, USA

8 * = corresponding author, raven@ucsb.edu
9

10 **Abstract**

11 In combination with dramatic and immediate CO₂ emissions reductions, net-negative atmospheric CO₂
12 removal (CDR) is necessary to maintain average global temperature increases below 2.0 °C. Many
13 proposed CDR pathways involve the placement of vast quantities of organic carbon (biomass) on the
14 seafloor in some form, but little is known about their potential biogeochemical impacts, especially at
15 scales relevant for global climate. Here, we evaluate the potential impacts and durability of organic
16 carbon storage specifically within deep anoxic basins, where organic matter is remineralized through
17 anaerobic processes that may enhance its storage efficiency. We present simple biogeochemical and
18 mixing models to quantify the scale of potential impacts of large-scale organic matter addition to the
19 abyssal seafloor in the Black Sea, Cariaco Basin, and the hypersaline Orca Basin. These calculations
20 reveal that the Black Sea in particular may have the potential to accept biomass storage at climatically-
21 relevant scales with moderate changes to the geochemical state of abyssal water and limited
22 communication of that impact to surface water. Many key unknowns remain, including the partitioning of
23 breakdown among sulfate-reducing and methanogenic metabolisms and the fate of methane in the
24 environment, which can be monitored in part via changes in alkalinity, DIC, and pH. Given the urgency
25 of responsible CDR development and the potential for anoxic basins to reduce ecological risks to animal
26 communities, efforts to address knowledge gaps related to microbial kinetics, benthic processes, and
27 physical mixing in these systems are critically needed.

28
29
30 **Plain Language Summary**

31 In addition to dramatically and immediately reducing CO₂ emissions, it has become necessary to actively
32 remove CO₂ from the atmosphere in order to avoid the worst effects of climate change and meet the goals
33 of the Paris Agreement. Several of the approaches that are currently being discussed to remove CO₂ from

34 the atmosphere involve trapping large amounts of CO₂ as organic carbon in plants or algae and then
35 storing that carbon in the deep ocean. Here we ask how this type of carbon storage would likely impact
36 the ecology and chemistry of deep ocean environments, depending on the amount of material placed and
37 its location. Within the limitations of these first simple calculations, we find that specific anoxic basins
38 like the Black Sea may have the potential to sequester climatically-relevant quantities of organic C for
39 more than 1,000 years with moderate changes to deep water chemistry. It is our aim that these results
40 motivate rigorous field and experimental studies to develop more nuanced models for the impacts of
41 carbon storage in locations like the Black Sea.

42

43 **Key Points**

44 Organic carbon sequestration may be relatively efficient in parts of the ocean without O₂ or complex
45 animal communities.

46 The Black Sea may have the potential to durably sequester climatically-relevant quantities of organic
47 carbon.

48 Research is urgently needed to better understand potential biomass degradation rates and the mixing and
49 transport of degradation products.

50

51

52

53

54 **1. Introduction**

55 Both dramatic, rapid CO₂ emissions reduction as well as enhanced atmospheric CO₂ removal are required
56 to limit average global temperature increases to 2.0 °C or below. This 2.0 °C is considered critical for
57 avoiding the most severe impacts of climate change (Armstrong McKay et al., 2022; IPCC AR6, 2021).

58 There is therefore a global need to develop a suite of atmospheric CO₂ removal (CDR) techniques that
59 operate at the gargantuan scale of excess anthropogenic CO₂ emissions while minimizing environmental
60 and social risks. Ocean biomass sequestration is one of the primary CDR strategies discussed in recent
61 strategy reports (National Academies of Science, Engineering, and Medicine, 2021) and can encompass a
62 wide range of techniques including enhanced upwelling, seaweed farming, and crop waste sinking, among
63 others. Each of these techniques presents a distinct suite of potential benefits and risks (Boyd et al., 2022),
64 but there has been minimal research to date into the likely impacts of deep ocean biomass sequestration

65 on the water column and seafloor (c.f., Ocean Visions and Monterey Bay Aquarium Research Institute,
66 2022). Deep benthic seafloor ecosystems remain largely unexplored, and we learn more each year about
67 their complexity and function (Orcutt et al., 2020). These seafloor environments are sensitive to the
68 changes in geochemical and physical conditions that could result from biomass storage (Levin et al.,
69 2023) in ways that are likely to vary substantially depending on local conditions.

70 In this contribution, we investigate the biogeochemical impacts of deep ocean biomass storage on or near
71 the seafloor, focusing on environments that lack the O₂ required to support a canonical animal community
72 or aerobic microbial respiration. We discuss differences between the biogeochemical processes that
73 control the efficiency of organic carbon storage in oxygenated (“oxic”) versus deoxygenated (“anoxic”)
74 environments, and we present calculations that constrain the potential biogeochemical impacts of biomass
75 storage in three well-studied anoxic basins on Earth today. We exclude issues related to the cultivation or
76 nutrient manipulation required for farming within the ocean, e.g., seaweed farming, such that our
77 approach is generalizable to any marine or terrestrial carbon source.

78

79 **2. Background**

80 **2.1 Organic carbon sequestration in oxic and anoxic environments**

81 Throughout Earth history, the enhanced burial of organic carbon in seafloor sediments has been one of the
82 principal mechanisms by which atmospheric CO₂ concentrations have declined from hothouse regimes.
83 The Ocean Anoxic Events (OAEs) of the Mesozoic provide particularly dramatic examples of this
84 phenomenon (Schlanger and Jenkyns, 1976; Jarvis et al., 2011; Owens et al., 2018). For example, during
85 the Late Cretaceous period, atmospheric CO₂ concentrations were near ~1400 ppm (Du Vivier et al.,
86 2015) and a particularly widespread ocean anoxia event (OAE-2, ~94 million years ago) facilitated the
87 burial of massive, organic carbon-rich deposits across the proto-North Atlantic (Sinninghe Damsté and
88 Köster, 1998; Raven et al., 2019). This 500,000-year-long burial event, representing an excess organic
89 carbon burial of $\sim 3 \times 10^{18}$ mol C (132,000 Pg CO₂), drove a global carbon-isotope excursion in the
90 residual marine DIC pool and is thought to have been so effective at reducing atmospheric CO₂ that it
91 caused the Plenus cold event (Jarvis et al., 2011; Owens et al., 2016; Kuhnt et al., 2017). In marginal
92 marine environments during OAE-2, local organic carbon accumulation rates of up to 2.15 g cm⁻² kyr⁻¹
93 were nearly 100x higher than modern averages for similar environments (Raven et al., 2019; Hülse et al.,
94 2021).

95 Critical environments for carbon burial during OAE-2 and other similar events typically have high
96 sedimentation rates, elevated local primary productivity, and limited O₂ penetration into sediment

97 porewaters (Hedges and Keil, 1995; Hartnett et al., 1998; Bianchi et al., 2018). In the absence of O₂,
98 microorganisms can respire organic carbon using alternative electron acceptors such as nitrate and sulfate
99 to break down many organic molecules, although certain (oxidized) molecules can become energetically
100 inaccessible at low Eh (Boye et al., 2017). Anoxic conditions also limit the functionality of oxidative
101 exoenzymes that rely on oxygen radicals or O₂ to generate small organic molecules (Sinsabaugh, 2010),
102 which can be subsequently consumed by single-celled organisms. Microbial sulfate reduction produces
103 sulfide, which can react with (sulfurize) certain functional groups in organic matter (Kohnen et al., 1990;
104 van Dongen et al., 2006; Raven et al., 2021) and contribute significantly to rates of organic carbon
105 preservation in sediments (Sinninghe Damsté and Köster, 1998; Raven et al., 2018; Hülse et al., 2019).
106 Together, these processes supported CO₂ sequestration as organic-rich shales in anoxic basins during
107 climatically sensitive intervals throughout Earth history and allowed these sedimentary rocks to serve as
108 efficient repositories for the sequestration of atmospheric CO₂ over geologic timescales.

109 Another important factor limiting rates of biomass breakdown in anoxic basins is the absence of most
110 eukaryotic organisms, including the vast majority of multicellular grazers. These organisms physically
111 mix surface sediments and degrade organics, thereby enhancing biomass breakdown (Aller, 1994; Aller
112 and Cochran, 2019). Although animals, e.g., nematodes, can survive periods of anoxia, anoxic conditions
113 preclude growth for all but the most specialized eukaryotes (Fenchel, 2012). Instead, the principal
114 organisms found in these basins are bacteria and archaea. Anaerobic fungi play a poorly constrained role
115 in anoxic marine environments, but least 18 genera of anaerobic fungi have been reported so far (Hess et
116 al., 2020), most of which are found in consortia with methanogenic archaea in animal gut and rumen
117 studies. Of relevance for potential CDR applications, the effective absence of animals in anoxic
118 environments means that human activities at the seafloor will not directly encounter complex animal
119 ecosystems (Levin et al., 2023).

120 Specific biomass breakdown rates are especially sensitive to changes in oxygenation and available
121 respiratory metabolisms. Generally speaking, aerobic and anaerobic microorganisms have the capacity to
122 respire certain highly labile compounds at similar rates (Lee, 1992). However, anaerobic organisms have
123 a limited capacity to metabolize more chemically resistant, recalcitrant molecules like lignins and other
124 structural polymers (Benner et al., 1986; Cowie and Hedges, 1992; Hulthe et al., 1998; Marchand et al.,
125 2005). Lignins are relatively oxidized compounds that represent a major proportion (often 15-35%) of
126 biomass in the woody materials of terrestrial plants (Li et al., 2016). In sediments, lignins are generally
127 resistant to rapid breakdown because specific steps in their degradation benefit from oxic exoenzymes
128 and/or physical feeding by metazoans (Marchand et al., 2005). Demethylation of lignins, or the
129 breakdown of methoxy (-OCH₃) side chains, can be achieved aerobically by some bacteria and fungi but

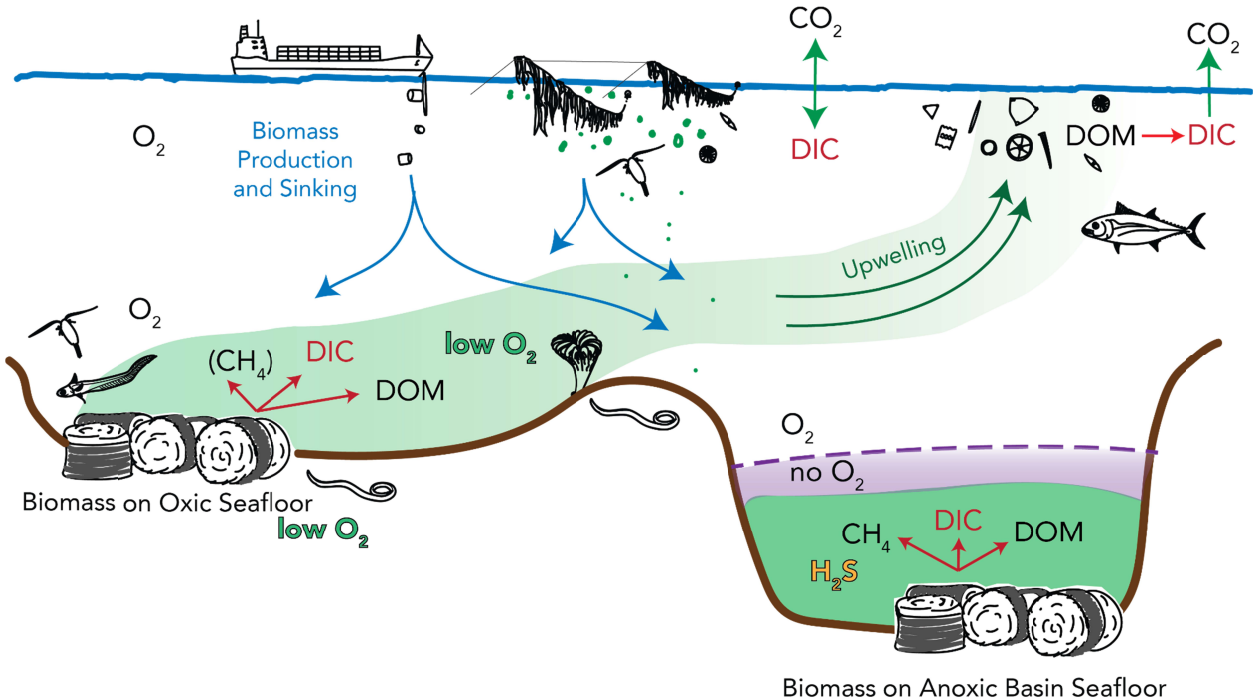
130 also anaerobically by sulfate-reducing, acetogenic, and fermenting bacteria as well as some methanogenic
131 archaea (Young and Frazer, 1987; Mayumi et al., 2016). The degradation of the remaining carbon in
132 lignin occurs in two major steps – the first, depolymerization, is the more chemically challenging step,
133 and the second is lignin monomer metabolism (Agarwal et al., 2018). Most organisms capable of this
134 depolymerization reaction (mainly fungi) use peroxidase enzymes that require oxic conditions. In the
135 absence of oxygen, for example in ruminant guts, some anaerobic fungi can perform the first steps in
136 lignin depolymerization and may partner with archaeal methanogens (Hess et al., 2020). In marine
137 environments, most lignocellulose breakdown is conducted by bacteria (Benner et al., 1986). Rates of
138 lignin degradation in anoxic marine systems are generally hard to detect (Benner et al., 1984; Keil et al.,
139 2010) and woody (lignin-rich) archaeological remains are famously well-preserved in the Black Sea
140 (Ballard et al., 2001). Although the consortia of organisms responsible for anaerobic lignin breakdown are
141 only partly understood, it would be reasonable to hypothesize that a fungus or bacteria+methanogen
142 consortium would be capable of conducting complete lignin degradation in anoxic marine basins at rates
143 that are significant but likely orders of magnitude slower than rates for other major biomass components.
144 Therefore, biomass that is rich in lignins and other oxidized structural polymers is likely to be especially
145 resistant to biological breakdown under anoxic conditions.

146

147 **2.2 Impacts of enhanced organic carbon addition to the seafloor**

148 Seafloor organic carbon storage may impact benthic environments, the mid-water column, and
149 ‘downstream’ regions such as upwelling zones (Siegel et al., 2021; Levin et al., 2023; **Fig. 1**). Most of
150 these risks stem from the breakdown of sequestered biomass by heterotrophic organisms to generate
151 dissolved species, including dissolved organic matter (DOM), CO₂ from respiration, or the products of
152 anaerobic metabolisms like sulfide (H₂S) and methane (CH₄). Each of these species can impact
153 downstream environments or modify the efficiency of carbon storage. CO₂ addition is a source of acidity
154 and its carbon can be returned to the atmosphere if the host water mass returns to the surface (Siegel et al.,
155 2021). Remineralized nutrients (e.g., ammonium, NH₄⁺) may enhance productivity in downstream
156 (surface) environments or drive changes in expressed anaerobic microbial metabolisms. The release of
157 DOM, depending on its composition, can stimulate bacterial communities and change the local ecological
158 structure (Boyd et al., 2022). DOM may also be a future source of CO₂ as it continues to degrade (Sexton
159 et al., 2011; Paine et al., 2021). Lowered O₂ concentrations threaten the growth of most aerobic organisms
160 and metazoans (Fenchel, 2012), although anaerobic microorganisms can still remineralize biomass by
161 respiring other electron acceptors such as nitrate, manganese and iron oxides, and sulfate, which leads
162 them to generate alkalinity, methane, reactive metals, and/or sulfide as well as CO₂ and DOM. After their

163 release, these dissolved compounds are transported away from seafloor installations by the general
 164 circulation around the sequestration site.



165
 166 **Fig. 1. Overview of potential outcomes for organic C sequestered in oxic and anoxic regions of the**
 167 **seafloor.** Red arrows indicate potential pathways for sequestered biomass transformations in the
 168 environment: respiration to dissolved inorganic carbon (DIC), fermentation to DIC and methane (CH₄), or
 169 breakdown to dissolved organic matter (DOM). Organic matter respiration in oxic environments
 170 consumes O₂, while OM respiration in anoxic environments generally consumes sulfate (SO₄) and
 171 releases sulfide (H₂S). In the open ocean, dissolved species return to the ocean surface on the timescales
 172 of ocean mixing (hundreds to thousands of years).

173
 174 The durability of ocean carbon storage therefore depends on the location (e.g. depth, environmental
 175 conditions, and downstream circulation) and form (overall recalcitrance) of organic carbon addition (**Fig.**
 176 **1**). In the case of the free, unballasted (slow) sinking of either micro- or macroalgae, large amounts of
 177 dissolved carbon will be generated in the deep thermocline and mid-water column as material sinks in the
 178 form of both CO₂ and dissolved organic matter (DOM) (Krause-Jensen and Duarte, 2016). Depending on
 179 their location, these relatively shallow water masses often upwell back to the surface and release any
 180 produced CO₂ on timescales of decades to hundreds of years. In contrast, packaged and ballasted or
 181 otherwise densified organics may be effectively stationary on the seafloor, and the abyssal (>2,000 m
 182 depth) water masses they encounter generally return to the surface and ventilate their CO₂ more slowly,

183 over hundreds to thousands of years (Siegel et al., 2021). The location of sequestered biomass is thus an
184 important determinant of the durability of sequestration on these longer timescales.

185 In sediments, degradation of overlying OM will cause biogeochemical effects that are similar to those
186 seen in the water column, but these effects are more locally concentrated near the sequestration site.
187 Organic matter accumulations will deplete electron acceptors in sediments, driving them toward more
188 reducing conditions (Froelich et al., 1979) and causing bacterial and archaeal heterotrophic communities
189 to adjust to favor anaerobic metabolisms. Seafloor communities may also be impacted by the introduction
190 of epibiotic organisms, viruses, or chemical species carried in with biomass materials (Fraser et al., 2011).
191 Locally elevated concentrations of organics may attract opportunistic scavengers to feed on the deposit.
192 Nevertheless, the scale and severity of ecological effects will depend on the seafloor region selected for
193 storage.

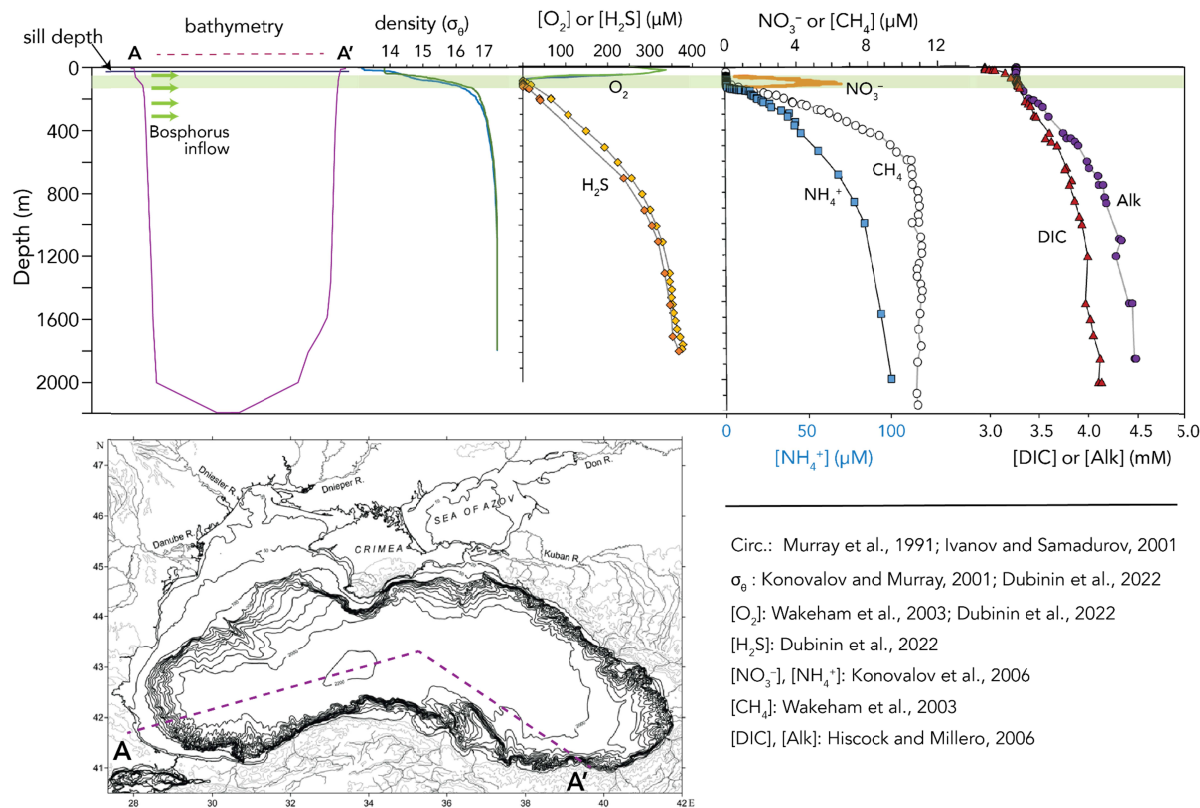
194 Below, we evaluate the potential impacts of biomass respiration on the biogeochemistry of deep anoxic
195 basins, focusing on cycles of carbon (CO_2 and CH_4), sulfur (SO_4^{2-} and H_2S), nitrogen (NH_4^+ and NO_3^-),
196 phosphate, alkalinity, and pH to inform a preliminary assessment of biogeochemical impacts and
197 ecological risks. Using published estimates of basin circulation and mixing parameters, we also assess the
198 durability of storage for dissolved biomass breakdown products in specific basins and estimate the
199 timescales over which dissolved species may impact the upper water column. Finally, we discuss the
200 potential capacity for major anoxic basins on Earth today – the Black Sea, Cariaco Basin, and Orca Basin
201 – to sequester organic carbon at climatically meaningful scales.

202

203

204 **2.3 Site Description: Modern anoxic basins**

205 **2.3.1 *Black Sea***



224 amounts of DIC (4,100 μM), ammonia (100 μM), phosphate (10 μM), alkalinity (4,400 μM), silica (350
225 μM) and DOC (0.5 mM) (Hiscock and Millero, 2006) (**Fig. 2**). Sulfide concentrations in the deep basin
226 have varied over time, with reported values ranging from 350– 440 μM (Konovalov and Murray, 2001;
227 Hiscock and Millero, 2006; Dubinin et al., 2022). Sulfide is a major contributor to the total alkalinity
228 budget in the deep Black Sea (Hiscock and Millero, 2006).

229 Especially since the mid-20th-century, the biogeochemistry of the Black Sea has been substantially
230 impacted by eutrophication, which provides an illustrative example of how the basin responds to changes
231 in organic matter flux. Between the 1960s and 1980s, enormous fluxes of agricultural nutrients drove a
232 more-than-doubling of primary productivity in the central Black Sea (Konovalov and Murray, 2001). This
233 excess organic carbon was largely remineralized in the upper water column by oxic respiration and, after
234 the depletion of available O_2 , via MSR, which produces sulfide. Eutrophication over this period has
235 caused sulfide production in the basin to roughly double, adding 0.13-0.22 Tmol excess $\text{H}_2\text{S}/\text{yr}$
236 (Konovalov and Murray, 2001). This substantial perturbation to the upper water column led to an
237 apparent shoaling of both the upper and lower interfaces of the sub-oxic zone (Konovalov 2001).

238 At moderate depths and especially near the shallow northwestern shelf, fluxes of organic matter to the
239 sediments of roughly 0.47 Tmol of organic carbon/yr (Dubinin et al., 2022) are often sufficient to exhaust
240 dissolved sulfate in pore water and drive methanogenesis (Reeburgh et al., 1991; Jørgensen et al., 2001).
241 Sediments from moderate depths in the Black Sea produce substantial amounts of methane, releasing
242 ~ 0.29 Tmol CH_4/yr to the basin, while abyssal sediments are thought to be sinks for methane overall
243 (Reeburgh 1991). Methane is also injected into the basin from point sources like seeps and methane
244 ‘volcanoes,’ which are concentrated at depths below 750 m. Total methane sources from seeps and other
245 point sources are estimated to be ~ 0.39 Tmol CH_4/yr (Schmale et al., 2011). Nevertheless, less than 1%
246 of the sedimentary methane released from both methanogenesis and point sources reaches the atmosphere
247 due to a combination of slow mixing and active anaerobic oxidation of methane (AOM) in the anaerobic
248 water column (~ 6 μM CH_4/yr) (Wakeham et al., 2003; Starostenko et al., 2010; Egorov et al., 2011;
249 Schmale et al., 2011). Anaerobic methane oxidation in the water column appears to follow roughly first-
250 order kinetics dependent on methane concentration, and water column communities of anaerobic archaea
251 can oxidize methane pulses efficiently (Wakeham et al., 2003; Schmale et al., 2011). Water column
252 methane concentrations are ~ 11 μM below 500 m and 10 nM at the surface (**Fig. 2**).

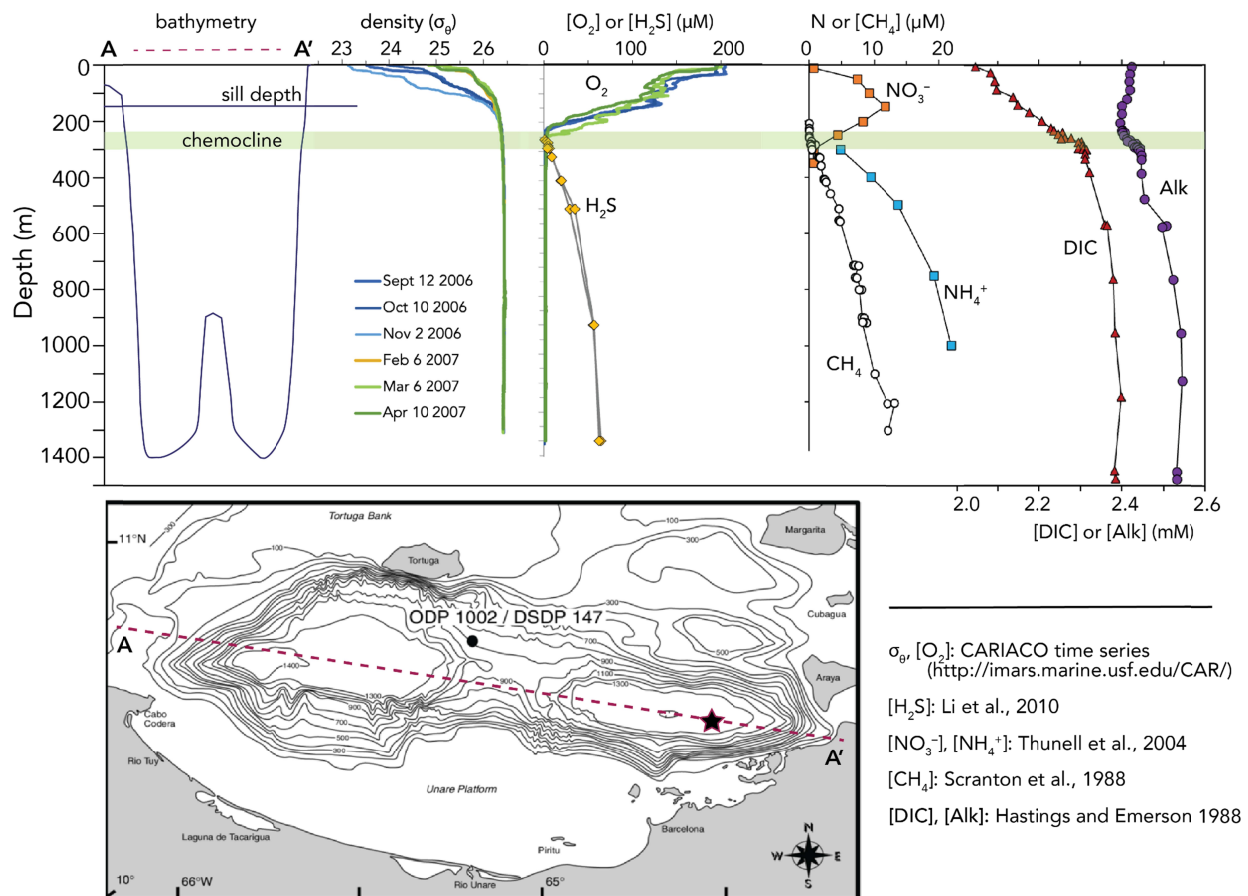
253 The abyssal Black Sea is characterized by a relatively well-mixed benthic boundary layer below ~ 1750 m
254 water depth (Murray et al., 1991), with a total volume of 75,137 km^3 . The top of this benthic boundary
255 layer is defined by the loss of a temperature gradient, and water exchanges slowly across this interface via
256 primarily diffusive processes (Murray et al., 1991). Water movement and density homogenization within

257 the deep boundary layer are driven by thermal convection (Ivanov and Samodurov, 2001), while mixing
 258 within the mid-water column are driven primarily by mesoscale cyclonic and occasional anticyclonic
 259 eddies (Markova, 2023). Currents in the deep Black Sea thus differ from the well-known rim current
 260 system in surface water.

261

262 2.3.2 Cariaco Basin

263 The Cariaco Basin is a 200-km-by-50-km trench located on the Venezuelan continental shelf that is
 264 separated from the Caribbean Sea by a sill at ~150 m water depth. Since roughly the end of the last glacial
 265 period, restricted circulation in the 1400 m-deep basin and high surface productivity have caused the
 266 basin water to be sulfidic below ~350 m depth. Cariaco Basin was the focus of an international long-term
 267 time series program from 1995 to 2017 (Muller-Karger et al., 2019), which provides a high-resolution
 268 record of the relationship between upwelling and productivity in the basin.



269

270 **Fig. 3: Cariaco Basin geochemistry.** The star on the map panel indicates the location of the CARIACO
 271 long-term time series station and profile site for all data except DIC/Alk. The cross-section A–A’ is 200
 272 km long.

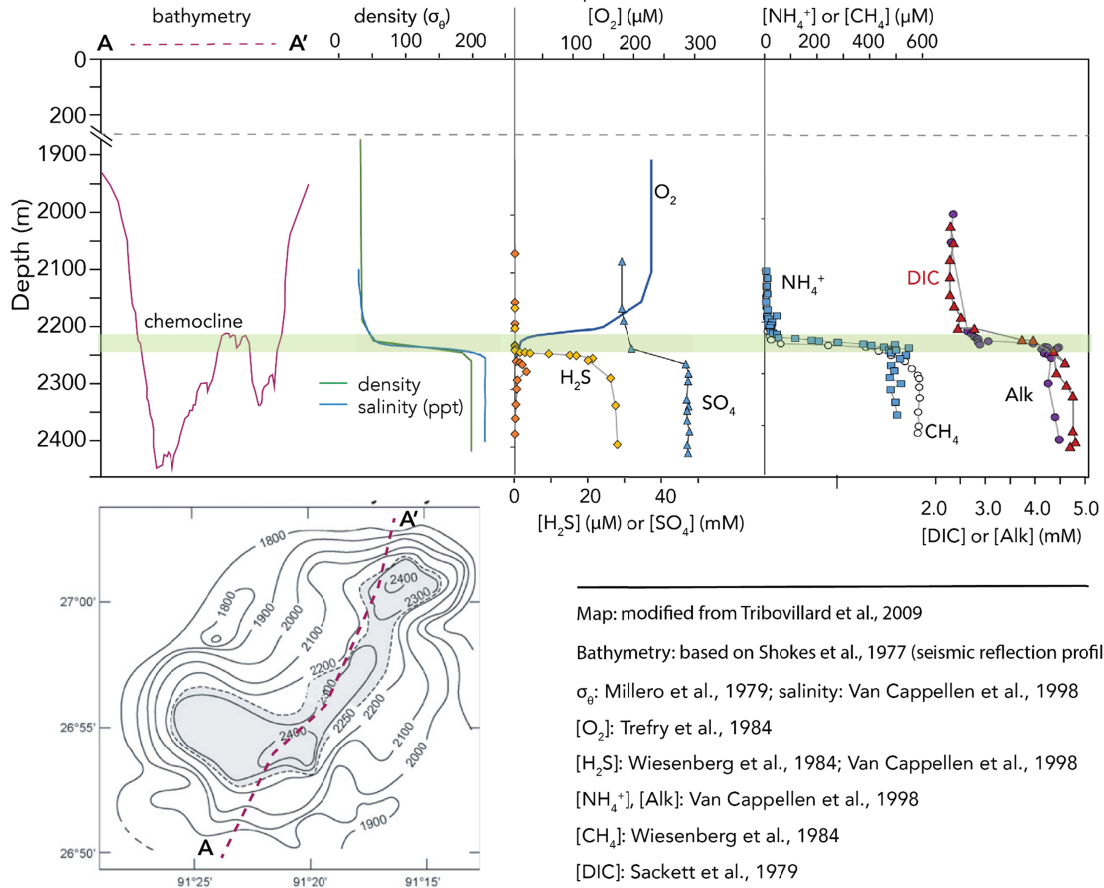
273 Cariaco Basin is more weakly stratified than the Black Sea and experiences seasonal upwelling (Muller-
274 Karger et al., 2004). The density gradient in the water column (**Fig. 3**) is driven entirely by a small
275 temperature differential from $\sim 18.1^{\circ}\text{C}$ at the surface to $\sim 16.8^{\circ}\text{C}$ at depth, while deep water is less saline
276 than surface water. Accordingly, eddy diffusion coefficients in eastern Cariaco Basin (Scranton et al.,
277 1987) are $\sim 30\times$ higher than those measured in the Black Sea, which means that dissolved components mix
278 toward the chemocline on much faster timescales. This temperature gradient is also not always stable, as
279 Scranton et al. (1987) noted significant warming from 1955-1982 and the basin may have experienced a
280 full overturn in the early 20th century (Zhang and Millero, 1993). Accordingly, concentrations of sulfide
281 in the deep basin do not appear to be in steady-state and may be reset by tectonic activity and associated
282 periodic intrusions of oxygenated seawater (Scranton et al., 2001).

283 Upwelling in the region drives elevated productivity and organic carbon export to the basin of about
284 $\sim 1 \times 10^{11}$ g C/yr (0.008 Tmol C/yr). In the sulfidic water column, most of this organic matter is respired via
285 sulfate reduction. In the sediments, estimated methane fluxes of roughly $10 \mu\text{mol cm}^{-2} \text{ yr}^{-1}$ (Scranton,
286 1988) suggests that at least 25% of the carbon delivered to sediments each year ($75\text{-}80 \mu\text{mol cm}^{-2} \text{ yr}^{-1}$;
287 Muller-Karger et al., 2004) is eventually consumed via methanogenesis, while 35% is consumed by
288 sulfate reduction and $\sim 40\%$ is preserved (Raven et al., 2016). Although a total of nearly 7.1×10^8 mol CH_4
289 yr^{-1} is produced in Cariaco sediments, roughly $\sim 85\%$ of this methane is oxidized in the anoxic water
290 column (Reeburgh, 1976; Scranton, 1988). In the deep basin, the approximately linear increase in
291 methane concentrations to $\sim 10 \mu\text{M}$ is thought to primarily reflect methane sourced from the sediments
292 (**Fig. 3**; Ward et al., 1987; Scranton, 1988).

293

294 2.3.3 *Orca Basin*

295 Orca Basin is a 200-meter-deep seafloor depression filled with anoxic, hypersaline water that underlies
296 $\sim 2,200$ meters of ‘normal’ oxygenated seawater in the Gulf of Mexico. The continental shelf bordering
297 Louisiana and Texas (USA) is pockmarked by many such basins, generally produced by the intersection
298 of tectonics and salt dissolution. The total volume of brine in Orca Basin is $\sim 10.24 \text{ km}^3$, and the basin
299 area at the permanent halocline is 158 km^2 (Diercks et al., 2019). The physical capacity of the basin for a
300 10-meter-thick idealized biomass layer is equivalent to $\sim 0.6 \text{ Pg CO}_2$ (14 Tmol C) as solids, ignoring any
301 consideration of ballast or physical containment.



302

303 **Fig. 4: Orca Basin geochemistry.** The cross-section A–A’ is approximately 28 km long.

304

305 Seawater in Orca Basin is extraordinarily salty (47–318 psu; 258 g/kg; Shokes et al., 1977) due to
 306 dissolution of an exposed salt layer on its north and southeast rims. Brines accumulate in the basin due to
 307 their very high densities (~1300 g/L) and turn over very slowly, on timescales of ~7,900 years (Addy and
 308 Behrens, 1980). The pycnocline at the top of the brine sits at 2220–2250 m depth and acts as a strong
 309 impediment to mixing in either direction. Sinking marine particles and materials transported from the
 310 Mississippi are suspended at this interface, where they age and become substantially degraded (Trefry,
 311 1984; Tribovillard et al., 2008; Diercks et al., 2019). Organic materials that do eventually sink into the
 312 dense brine produce OC-rich soupy muds that continue to be degraded slowly by sulfate-reducing and
 313 methanogenic microorganisms (LaRock et al., 1979; Hurtgen et al., 1999; Nigro et al., 2020).

314 Due to this long, gradual accumulation of OM breakdown products, Orca Basin brines are rich in DOM
 315 (89–278 μM or 2.5×10^9 mol C total; Diercks et al., 2019). Sulfate concentrations are high throughout the
 316 basin and exceed 40 mM in porewater throughout the upper 30 cm of sediments (Hurtgen et al., 1999).
 317 Although microbial sulfate reduction is active in the basin, iron concentrations are high and react

318 efficiently with sulfide to generate iron monosulfides. Reported concentrations of dissolved sulfides
319 differ; maximum concentrations of 2-3 μM were reported within a narrow layer within the water column
320 during two cruises in the late 1970s (Wiesenburg et al., 1985), while Van Cappellen et al. (1998) reported
321 10 to 28 μM sulfide in all samples with salinities above 200 ppm. Microbes use iron and manganese
322 oxides in the upper pycnocline at 2200-2240 m depth (Van Cappellen et al., 1998), and iron sulfides
323 precipitate at the interface between regions of active iron and sulfur cycling (Sheu and Presley, 1986).

324 Despite high concentrations of available sulfate and the observation that hypersaline conditions do not
325 appear to limit MSR (Porter et al., 2007), methanogenesis is an active pathway of OM breakdown in the
326 Orca Basin. Methanogens in this environment appear to use ‘non-competitive’ methylated substrates for
327 methylotrophic methanogenesis, producing ^{13}C -depleted methane concurrent with MSR (Zhuang et al.,
328 2016). Methane and other biogenic hydrocarbons accumulate to high concentrations (up to 3.4 mM CH_4)
329 within the brine (Wiesenburg et al., 1985; Zhuang et al., 2016). Most of this methane is trapped by the
330 lack of mixing across the pycnocline, but methane that does mix into overlying waters is likely to be
331 oxidized by microbial communities in the overlying oxic waters of the Gulf of Mexico, which appear to
332 be highly effective at methane oxidation and are primed from abundant petroleum seep sources (Kessler
333 et al., 2011).

334

335 **3. Methods**

336 **3.1 Organic matter stoichiometry**

337 We estimate geochemical impacts on the mixed volume of each basin using a range of stoichiometries for
338 organic matter breakdown that represent end-member compositions for carbohydrate-rich and lipid-rich
339 biomass (Redfield, 1934; Anderson and Sarmiento, 1994), with and without ammonium reoxidation to
340 nitrate (Hastings and Emerson, 1988). In terms of their impacts on pH, DIC, alkalinity, and sulfide,
341 terrestrial biomass sources are approximated by the carbohydrate-rich end member; terrestrial materials
342 with lower N:C ratios would make calculated NH_4^+ concentration changes overestimates. We first
343 consider a case in which all biomass breakdown occurs via microbial sulfate reduction (MSR), which
344 oxidizes biomass to CO_2 and nutrients while reducing sulfate to sulfide. Unlike oxic respiration, microbial
345 sulfate reduction is a source of alkalinity, so its impact on pH is relatively small (Lyons et al., 1984).
346 However, the precise ratio of total alkalinity (TA) to DIC produced during organic matter
347 remineralization depends on the identity of the organic electron donor and its oxidation state (Gallagher
348 et al., 2012); more reduced organic compounds like lipids ($\sim\text{CH}_2$) require more oxidizing power to
349 generate CO_2 than more oxidized compounds like carbohydrates ($\sim\text{CH}_2\text{O}$). We convert widely used

350 literature estimates for $\Delta\text{CO}_2 : \Delta\text{O}_2$ into ratios of $\Delta\text{CO}_2:\Delta\text{SO}_4$ ratios by balancing electrons for each half
 351 reaction (Froelich et al., 1979; Middelburg et al., 2020). We also consider a case in which methanogenesis
 352 accounts for 10% of total organic C remineralization. In our simplified model, methanogenesis converts
 353 organic C to methane (CH_4) and CO_2 in a ratio that depends on the oxidation state of the organic C. This
 354 reaction does not produce alkalinity and therefore, in the absence of anaerobic methane reoxidation, has a
 355 relatively large effect on local pH. We present this full range of stoichiometries and metabolisms based on
 356 five scenarios (Table 1).

	Scenario	Organic Matter	Breakdown Products	$\Delta\text{DIC} :$ ΔAlk
1	Lipid-rich OM breakdown via MSR	$\text{C}_{117}\text{N}_{16}\text{P}$	$117\text{CO}_2 + 16\text{NH}_4^+ + \text{H}_2\text{PO}_4^- + 85\text{H}_2\text{S}$	+117:+170 (1:1.45)
2	Carb-rich OM breakdown via MSR with ammonium ox.	$\text{C}_{106}\text{N}_{16}\text{O}_{42}\text{H}_{175}\text{P}$	$106\text{CO}_2 + 16\text{NO}_3^- + \text{H}_2\text{PO}_4^- + 69\text{H}_2\text{S}$	+106:+122 (1:1.15)
3	Carb-rich OM breakdown via MSR without ammonium ox.	$\text{C}_{106}\text{N}_{16}\text{O}_{42}\text{H}_{175}\text{P}$	$106\text{CO}_2 + 16\text{NH}_4^+ + \text{H}_2\text{PO}_4^- + 53\text{H}_2\text{S}$	+106:+106 (1:1)
4	Lipid-rich OM breakdown via methanogenesis	$\text{C}_{117}\text{N}_{16}\text{P}$	$32\text{CO}_2 + 85\text{CH}_4 + 16\text{NH}_4^+ + \text{H}_2\text{PO}_4^-$	+32:+1
5	Carb-rich OM breakdown via methanogenesis	$\text{C}_{106}\text{N}_{16}\text{O}_{42}\text{H}_{175}\text{P}$	$53\text{CO}_2 + 53\text{CH}_4 + 16\text{NH}_4^+ + \text{H}_2\text{PO}_4^-$	+53:+1

357 **Table 1.** Reaction stoichiometries used for organic matter compositions and breakdown pathways.
 358 Balanced reactions linking organic matter to its products require H_2O and H^+ (not shown). OM = organic
 359 matter; MSR = microbial sulfate reduction.

360

361 All pH calculations were conducted using CO2SYS v.2.3, which accounts for sulfide, ammonia, and
 362 silicic acid alkalinity. Our analysis includes the linked cycles of carbon, nitrogen, phosphorus, sulfur, and
 363 alkalinity, but it excludes any interactions with iron or manganese cycling and the effects of organic acids.

364 Basin volumes were calculated in MATLAB R2018B using the trapz function at the 1 arcsecond
 365 resolution specified in the GEBCO 2022 bathymetry. In the abyssal Black Sea, although vertical mixing
 366 is relatively well constrained, very little data has been collected relevant to lateral mixing (Stanev et al.,
 367 2021). Therefore, as a first calculation, we focus only on the western portion of the Black Sea, and we
 368 mix the products of microbial reactions into a volume equivalent to 43% of the benthic boundary layer
 369 between 1750 m and the seafloor (Murray et al., 1991) to account for these uncertainties in lateral mixing.
 370 For Cariaco Basin, we calculated the volume of water in the eastern and western sub-basins separately as

371 well as the overlying seawater to 350 m, following observed concentration patterns in (Scranton et al.,
372 2001). For Orca Basin, products are mixed into a volume of 10.3 km³ (Diercks et al., 2019).

373

374 3.2 Circulation Model

375 Dissolved products of MSR will not be confined to the deepest layers of the water column. For the Black
376 Sea and Cariaco Basin, we use published estimates for advective flow and eddy (turbulent) diffusivity to
377 estimate vertical mixing and transport. In each case, we constructed a model composed of 0.1-km-thick,
378 vertically stacked layers following Scranton et al., (1987) and Schmale et al., (2011). The general
379 equation for this calculation is:

$$380 \frac{d[C]}{dt} = K_i * ([C]_{i-1} - [C]_i) * A_i / (V_i * \Delta z_i) + K_{i+1} * ([C]_{i+1} - [C]_i) * A_i / (V_i * \Delta z_i) + T_B * ([C]_B - [C]_i) / V_i$$

382 where [C] represents the concentration of any component, the subscript 'i' refers to a depth box, T
383 represents advective flow in km³/yr across the box boundary, z is box thickness (0.1 km), A and V are the
384 area and volumes of each box boundary in km² and km³ respectively, and K is eddy diffusivity in km²/yr.

385 In the deep Black Sea, estimates for eddy (turbulent) diffusivity are lower than for most open-ocean sites,
386 ranging from 4.1x10⁻⁴ to 1.2x10⁻⁴ km²/yr, equivalent to 4x10⁻⁶ to 1.3x10⁻⁵ m³/sec (Ivanov and Samodurov,
387 2001). The box model for the Black Sea uses 20 vertically-stacked, 0.1-km-thick layers (Schmale et al.,
388 2011) to evaluate the timescales over which dissolved products of deep biomass respiration might impact
389 the upper water column of the Black Sea. Below ~500 m depth in the Black Sea, transport is generally
390 limited to turbulent diffusion (K_i). In the upper 500 m, each box receives advective flow from the
391 Bosphorus with return via upwelling (T_B) and outflow from the surface box (Schmale et al., 2011). The
392 model is run with a one-year timestep for 1,200 years.

393 In Cariaco Basin, intermittent upwelling and a weak density gradient lead to higher estimates of eddy
394 turbulent diffusivity than for the Black Sea, ranging from 1.3x10⁻² to 2.7x10⁻³ km²/yr (Scranton et al.,
395 1987). The box model for Cariaco Basin uses 12 vertically-stacked, 0.1-km-thick layers and is run with
396 12 time steps per year for 200 years.

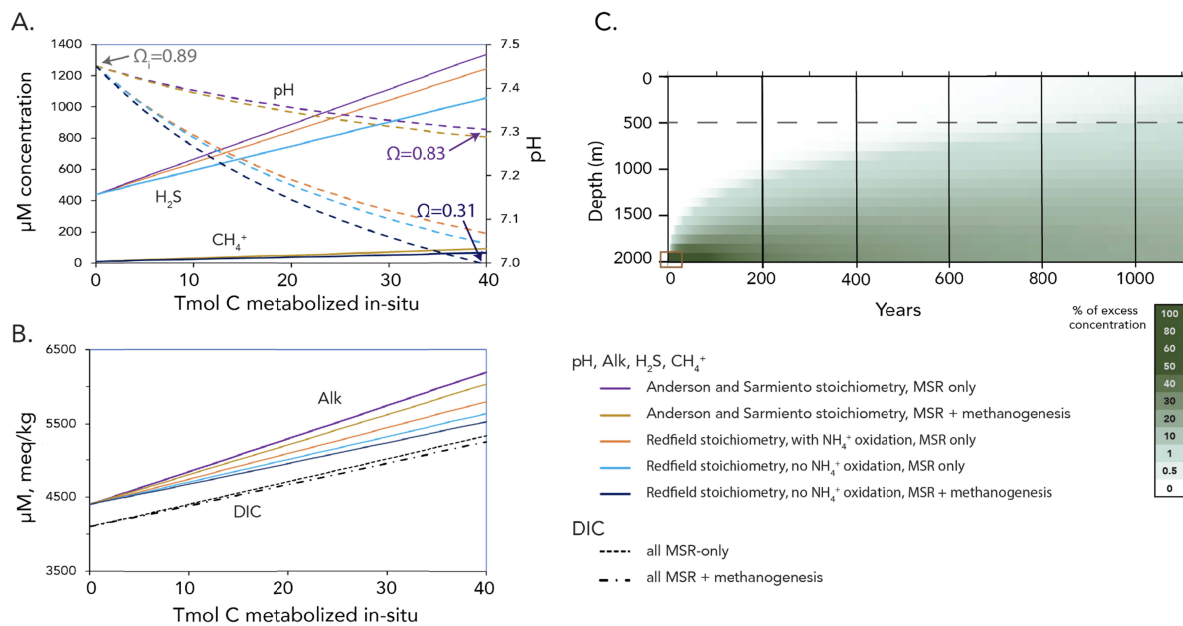
397

398 4. Results and Discussion

399 4.1 The Black Sea: Biogeochemical impacts of organic matter sequestration

400 We estimated the potential short-term (decadal) impacts of biomass addition to the deepest part of the
401 western Black Sea using the scenarios defined in Table 1. To calculate the effects of mixing organic

402 matter remineralization products into this environment, we use a volume of 32,398 km³, which is
 403 equivalent to ~43% of the total volume of the abyssal benthic boundary layer (75,137 km³). This reduced
 404 effective volume is an attempt to account for incomplete lateral mixing at depth and can be refined by
 405 future studies of advective flow dynamics within the layer (Markova, 2023). The amount of organic
 406 matter respired *in situ* over short (decadal) timescales was varied from 0 to 40 Tmol C, which is
 407 equivalent to 0–1.76 Pg (Gt) CO₂. Initial Black Sea deep water concentrations (NH₃ = 100 μM, H₂S = 440
 408 μM, TA = 4400 μM, DIC = 4100 μM) were taken from Hiscock and Millero (2006) and Dubinin et al.
 409 (2022). Salinity (22 psu) and temperature (8°C) were taken from Murray et al. (1991) (**Fig. 2**).



410
 411 **Fig. 5 Impacts of enhanced organic matter breakdown in abyssal western Black Sea water.** **A** –
 412 Calculated changes in pH (dashed lines), and sulfide and methane concentrations (solid lines) resulting
 413 from *in-situ* respiration of organic C by MSR, with or without methanogenesis, for a range of organic
 414 matter stoichiometries (Table 1). In scenarios 4 and 5, methanogenesis is presumed to metabolize 10% as
 415 much organic C as MSR. Annotations show the saturation state (Ω) of calcite (CaCO₃), which is
 416 undersaturated throughout. **B** – Associated changes in abyssal Black Sea DIC and alkalinity
 417 concentrations. **C** – Modeled vertical mixing of a dissolved component (HS⁻, HCO₃⁻, NH₄⁺ etc) added to
 418 the Black Sea at >2,000 m depth. Water depths above the dashed horizontal line experience advective
 419 flow.

420
 421 If we consider only the effects of biomass respiration by MSR, ignoring methanogenic metabolisms and
 422 subsequent reactions (e.g., sulfide oxidation; scenarios 1–3 in Table 1), we estimate that the microbial

423 respiration of 40 Tmol C below 2,000 m water depth would increase sulfide concentrations from a current
424 value of 440 μM to 1057–1337 μM , depending on mean organic C redox state (**Fig. 5**). Concurrently, in
425 the absence of ammonium oxidation, ammonium concentrations would increase from 100 μM to 279–296
426 μM . Because MSR generates alkalinity as well as CO_2 , the pH change associated with this breakdown
427 would be $\sim 0.15 - 0.41$ pH units. This is in notable contrast to the oxic respiration of this same quantity of
428 organic matter, which would cause pH to drop by more than 1 unit to a pH value of ~ 6.56 (calcite Ω
429 ~ 0.12) due to the absence of MSR-derived alkalinity. The deep Black Sea is currently undersaturated with
430 respect to calcite and aragonite, and therefore seafloor carbonates are minor and unlikely to substantially
431 buffer, or be substantially impacted by, changes in pH at this depth. At even larger scales, the addition of
432 100 Tmol C (1.2 Pg C) respired via MSR *in situ* would raise deep-water sulfide concentrations to nearly
433 2,000 μM (from 400 μM) and drop pH to 6.87 (from 7.40).

434

435 Biomass breakdown may also occur via methanogenic metabolisms. More experimental data is needed to
436 constrain the contribution of methanogenesis to biomass breakdown, which is likely to depend on both
437 biomass type and on the engineered specifics of any proposed CDR operation (i.e., compression,
438 containment, and placement of biomass). Canonically, methanogenesis is repressed in the presence of
439 sulfate due to the slight energetic favorability of MSR (Froelich et al., 1979; Kristjansson et al., 1982).
440 The overall effect of MSR-driven breakdown on basin dissolved sulfate concentrations is small, but
441 sulfate may nonetheless be locally depleted, especially within interiors of sunken biomass or within
442 underlying sediments. Even when sulfate is present, however, methanogenic organisms are frequently
443 capable of operating alongside sulfate reducers using ‘non-competitive’ substrates like methanol or
444 methylamine (Oremland and Polcin, 1982; Zhuang et al., 2016); lignin methoxy groups can also fall into
445 this category (Hess et al., 2020). Additional data are needed to partition likely biomass breakdown for
446 deep Black Sea conditions into MSR and methanogenesis under a range of engineering conditions and
447 placement scenarios.

448 We calculate the effects of methanogenesis on abyssal Black Sea geochemistry through Scenarios 4 and
449 5, both of which make the assumption that 10% of total organic C breakdown moves through this
450 pathway and exclude the potential later reoxidation of methane. For the same scale of total C respiration
451 discussed above (40 Tmol C), the addition of 2–2.9 Tmol CH_4 would increase abyssal methane
452 concentrations from current values of ~ 10 μM to 71–100 μM and add the equivalent of roughly 10–15 yrs
453 of natural CH_4 production in the shelf and slope sediments of the Black Sea (Reeburgh et al., 1991).
454 Organic matter breakdown in these scenarios leads to slightly larger changes in abyssal pH and saturation
455 state than MSR alone (Fig. 5) because methanogenesis does not produce alkalinity, unlike MSR.

456 However, if the methane produced during methanogenesis is subsequently reoxidized anaerobically with
457 sulfate, the summed reactions produce a net effect similar to breakdown via MSR alone (Middelburg et
458 al., 2020).

459 One critical question impacting the feasibility of anoxic organic matter sequestration is the ability of local
460 microbial communities to conduct anaerobic methane oxidation in the water column, removing methane
461 from the system before it can escape to the atmosphere. Natural methane sources in the shelf and slope
462 sediments of the Black Sea are large – approximately 0.29 Tmol CH₄/yr (Reeburgh et al., 1991; Schmale
463 et al., 2011) – and they are frequently local and episodic due to seafloor tectonic and other processes.
464 Methane sinks balance these inputs, largely through methanotrophy (methane oxidation) in the anoxic
465 water column of 1 to several hundred nM CH₄/day and CH₄ fluxes into abyssal sediments (Reeburgh et
466 al., 1991; Schmale et al., 2005). Studies in the similarly methane-rich Gulf of Mexico have observed 100-
467 fold increases in methanotrophy rate constants in response to methane injection from the Deepwater
468 Horizon oil spill (Kessler et al., 2011), and it has been argued that rates of Black Sea methanotrophy
469 could respond similarly, given sufficient time for the methanotrophic community (with a doubling time of
470 several months, Nauhaus et al., 2007) to grow (Schmale et al., 2011). Schmale et al. (2011) modeled the
471 fate of the instantaneous injection of 11.2 Tmol CH₄ at 2,000 m water depth in the Black Sea (e.g., due to
472 mid-depth hydrate destabilization or deep mud volcano eruptions) and concluded that this injection would
473 cause a negligible 2–3% increase in the total modern Black Sea flux of methane to the atmosphere due to
474 responsive rates of methanotrophy in the environment. Methanotrophy rates are also likely to show a
475 positive relationship with increased methane concentrations as current methane concentrations in the
476 Black Sea are near minimum thresholds for the activity of anaerobic methane oxidation (Valentine, 2011).
477 Additional work is needed to validate these model results and better understand the capacity of these
478 microbial methane oxidation processes to ‘scrub’ excess methane from the system.

479 Potential impacts of biogeochemical change in the abyssal Black Sea on human endeavors in the region
480 are highly sensitive to the mixing, or lack thereof, between abyssal waters and the surface. The Black Sea
481 is notably stratified, with minimal tidal action to add energy to the system (Stewart et al., 2007). We used
482 estimates of eddy diffusivity (Ivanov and Samodurov, 2001) from water column profiles to calculate the
483 rates at which dissolved products of organic C breakdown in the benthic boundary layer could be detected
484 near the shallow redoxcline (~150 m depth). As shown in Fig. 5, dissolved components added to deep
485 water from biomass respiration can remain contained within >500 m-deep, slowly ventilating water
486 masses over hundreds of years. As a percentage of the initial excess concentration in the deepest box, the
487 excess concentration in the 500-m-deep water column box is approximately 0.04% after 400 yrs, 0.25%
488 after 600 yrs, 0.83% after 800 yrs, and 1.26% after 1,000 yrs. For a scenario with 40 Tg C addition and

489 600 μM initial excess sulfide in the deepest box, this would be equivalent to an increase in the
490 concentration of sulfide at 500 m depth by 7.6 μM , or roughly 5% of current concentrations, after 1,000
491 years. From the perspective of the upper, upwelling water column, impacts of dissolved species are within
492 the range of natural variability (e.g. (Konovalov and Murray, 2001; Dubinin et al., 2022) for >1,000
493 years, assuming a roughly steady-state circulation in the Black Sea.

494 Although much of the energy from respiration of biomass is conserved in the short term, it will eventually
495 contribute heat to the system that could impact deep vertical stratification of the water column. If we
496 assume a rough energy yield of ~ 25 kJ/mol for MSR, the respiration of 40 Tmol C would generate $\sim 10^{15}$
497 kJ, which, if released over very short timescale of ten years, could be a significant fraction of the natural
498 geothermal heat flux driving convection in the benthic boundary layer of 0.04 W/m² (Zolotarev et al.,
499 1979), or 5.5×10^{15} kJ per decade. Changes in total energy flux and resulting water column stratification
500 from metabolic processes could therefore become relevant for a hypothetical case of very large-scale,
501 rapid implementation, but are otherwise unlikely to be significant.

502 All of the foregoing calculations focus solely on the products of *in situ* biomass respiration. Depending on
503 the timescale being considered and the composition of sequestered biomass, respired C will represent
504 some fraction of the total organic C added to the system. Initial experiments indicate that roughly 75% of
505 lignin-rich terrestrial biomass may persist after 100 years of sedimentary storage under partially
506 oxygenated conditions, and the efficiency of biomass storage is expected to be higher under anoxic
507 conditions (Keil et al., 2010). For a range of possible storage efficiencies between 50% and 85%, the *in*-
508 situ respiration of 40 Tmol C discussed above translates into a total sequestrations of 3.5 to 11.7 Pg (Gt)
509 CO₂ equivalent. In such a hypothetical scenario, carbon would be stored in two distinct pools: 50-90% of
510 sequestered carbon would be stored semi-permanently as solid biomass while 10–50% would be
511 sequestered on a kyr timescale as either dissolved CO₂ or DOM. In terms of the physical size of such an
512 installation, consolidated terrestrial biomass equivalent to 10 Pg CO₂ would, if deposited in a four-meter-
513 thick layer in the deepest region of the western Black Sea, cover 6,170 km², or 3.5% of the >2,100-m
514 seafloor (1.9% of total Black Sea area, an 80 x 80 km operation). The upper end of this range – a total
515 amount, not an annual flux – is an enormous value, similar to the total production of crop waste across the
516 entire planet in a year.

517 This highly simplified mass balance exercise suggests that the bulk geochemistry and stratification of the
518 Black Sea may allow for moderate changes in the concentrations of H₂S, NH₄, alkalinity, and pH to result
519 from the seafloor storage of a climatically relevant quantity of carbon. The scenario involving the *in-situ*
520 respiration of ~ 40 Tmol C that we use for discussion purposes here is of the same order of magnitude in
521 terms of increased organic C input as the 20th-century eutrophication of the Black Sea (Konovalov and

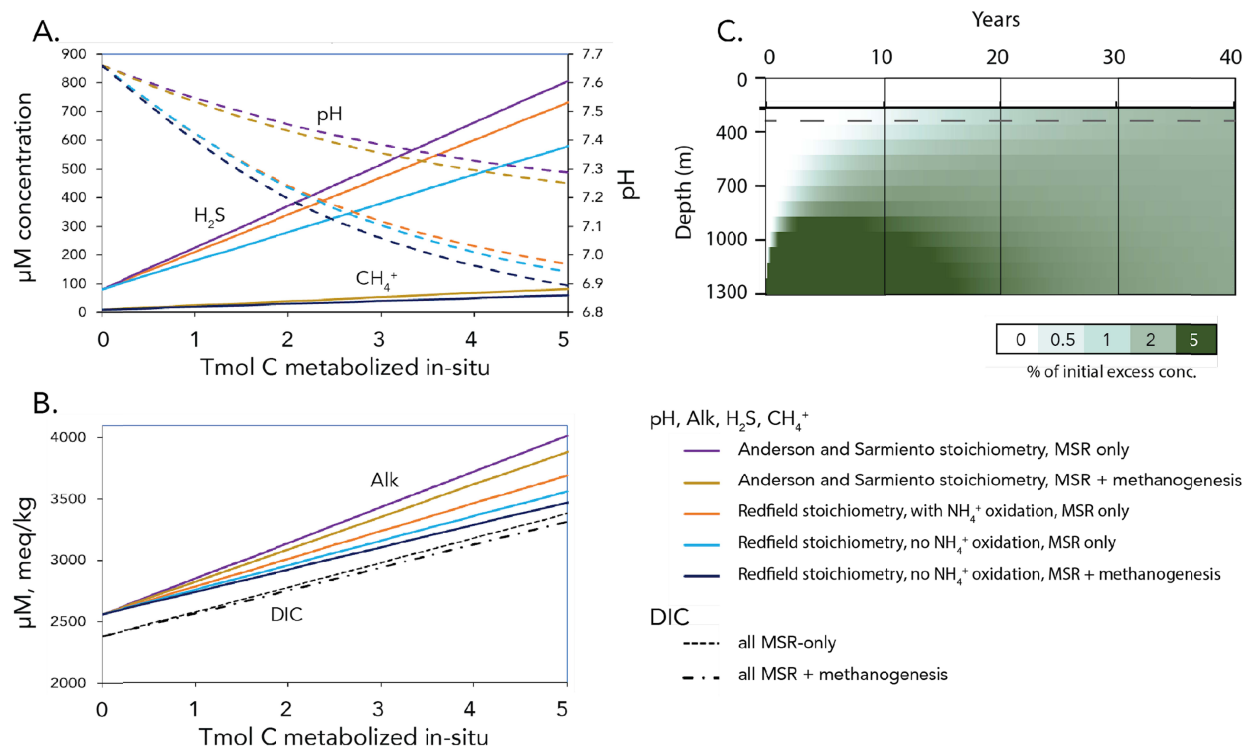
522 Murray, 2001). Importantly, however, biomass breakdown in abyssal waters has a diluted and delayed
523 effect on chemocline and mixed layer properties relative to shallow biomass breakdown. Geochemical
524 changes within the basin are also isolated from the global ocean by the singular connection at the
525 Bosphorus. This physical restriction provides spatial bounds for monitoring and verification of any CO₂
526 removal activities and isolates its impacts to a relatively well-defined set of stakeholders in the region.

527 Despite the potential for gigatonne-scale CO₂ sequestration suggested by these broad calculations, we
528 emphasize that this preliminary analysis has many limitations and also identifies potential risks that will
529 require additional research. We assume that remineralization products mix rapidly within a volume
530 equivalent to slightly less than half of the entire deep benthic boundary layer, neglecting acute or local
531 impacts, which may be especially important for predicting sedimentary methane production. We do not
532 explicitly consider reactions that re-oxidize sulfide or methane, and we do not yet have the experimental
533 data to support precise predictions of biomass consumption via methanogenesis or methane reoxidation
534 via methanotrophy. We also lack the necessary data to evaluate how seafloor heterotrophic communities –
535 bacteria, archaea, and potentially fungi – will respond to a massive influx of biomass in this environment.
536 And finally, more data is needed to constrain physical mixing and circulation within the deep Black Sea
537 benthic boundary layer. It is our aim that these results motivate rigorous field and experimental studies to
538 develop more nuanced models for the durability and ecological impacts of biomass storage in the Black
539 Sea.

540

541 **4.2 Cariaco Basin: Biogeochemical impacts of organic carbon sequestration**

542 Using the same general approach and stoichiometric scenarios (Table 1) that we used for the Black Sea,
543 we estimated the potential effects of biomass addition to the deep seafloor of Cariaco Basin. The amount
544 of organic matter respired in situ was varied from 0 to 5 Tmol C, and initial geochemical conditions for
545 the deep Basin are summarized in Figure 2.



546
 547 **Figure 6. Effects of enhanced OM breakdown on Cariaco Basin water chemistry** below 350 m water
 548 depth, based on scenarios in Table 1. In scenarios 4 and 5, methanogenesis is presumed to metabolize
 549 10% as much organic C as MSR. **A** – Concentrations of sulfide or methane (solid lines) following various
 550 scenarios; sulfide concentrations in MSR-only scenarios 1 and 4 are the same for mixed-metabolism
 551 scenarios 2 and 5, respectively. **B** – Concentrations of DIC (dashed) and alkalinity (solids) following
 552 various scenarios. **C** – Mixing of dissolved species in the western Cariaco Basin over several decades.
 553 Calculations conservatively use eddy diffusion coefficients from Scranton (1987), although these lead to
 554 ~10x faster mixing than the values assumed by earlier work (Fanning and Pilson, 1972; Reeburgh, 1976).

555
 556 The vertical circulation and mixing timescale of Cariaco Basin are very different from the case of the
 557 Black Sea. Cariaco Basin is relatively well mixed below the chemocline at 350 m depth but is divided
 558 into eastern and western sub-basins that lack lateral mixing. Given seasonal upwelling and weak
 559 stratification in the basin, dissolved species from the deepest part of the basin reach the chemocline depth
 560 within about 20 years (**Fig. 6**). Accordingly, to assess the geochemical impacts of CDR-scale biomass
 561 addition, we calculated potential changes in deep water chemistry for this full volume of ~5,000 km³. The
 562 remineralization of 2 Tmol of organic C in this volume increases modeled sulfide concentrations from an
 563 initial value of 80 μM to 262–375 μM , depending on the stoichiometry of the organic matter source and

564 the metabolic pathways used (scenarios 1–5). This amount of remineralization would also cause increases
565 in NH_4^+ (from 20 μM to 75–82 μM) and CH_4 (from 10 μM to 28–36 μM). The appearance of excess
566 sulfide and ammonium at the chemocline will enhance O_2 demand and may shoal the water column oxic-
567 anoxic interface. More complex modeling efforts will be required to assess these dynamic interactions
568 and the many linked redox reactions they impact near the chemocline.

569 The pH change associated with the in situ remineralization of 2 Tmol of relatively reduced (lipid-rich)
570 organic carbon (scenarios 1 and 4) is ~ 0.2 units (from 7.66 to 7.45), while the pH change for more
571 oxidized organic carbon (scenarios 2, 3, and 5) is 0.43 units (from 7.66 to 7.23). Unlike the Black Sea, the
572 deep Cariaco Basin is supersaturated with respect to CaCO_3 (calcite $\Omega = 1.79$). The larger pH change
573 associated with scenarios 2, 3, and 5 would drive calcite to be undersaturated ($\Omega = 0.77$), favoring
574 dissolution (**Fig. 6**). Actual pH change would be strongly buffered by reactions with highly abundant
575 carbonates in Cariaco Basin sediments (Aguilar et al., 2017).

576 The effectiveness of Cariaco Basin as a site for biomass storage and CDR is far more sensitive to the
577 efficiency of biomass breakdown than the Black Sea because its weak density gradient and history of
578 dynamic redox change raise the possibility of deep mixing and ventilation. Key targets for future research
579 include this biomass breakdown efficiency and its trajectory over time, as well as understanding the
580 responsiveness of water column methane oxidizing organisms to changes in methane flux. Using a range
581 of estimates for terrestrial biomass storage efficiencies over several decades of 50–85% (Keil et al.,
582 2010), the in-situ respiration of 2 Tmol C could represent a total initial carbon sequestration of 0.18–0.59
583 Pg CO_2 equivalents, with part stored as solid-phase bales stable over centennial timescales and the
584 remainder present dissolved species with lower durability. In this scenario, this quantity of baled biomass
585 would physically fill the lowest part of the western sub-basin (>1236 m depth, 1500 km^2 area, Scranton,
586 1988) to an average thickness of roughly 2.7 m. Establishing acceptable limits for environmental change
587 requires collaboration by many stakeholders, most critically the local Venezuelan communities that are
588 economically invested in both fisheries and any future CDR industry. As a first-order evaluation to guide
589 this multi-stakeholder decision making, however, Cariaco Basin appears to have sufficient
590 biogeochemical capacity to support meaningful quantities of biomass carbon storage and is deserving of
591 further research attention, most importantly to address uncertainties related to upwelling and storage
592 durability.

593

594 **4.3 Orca Basin and other hypersaline basins**

595 Orca Basin is much smaller than either the Black Sea or Cariaco Basin, with a total brine volume of just
596 10.2 km^3 (compared to $5,000 \text{ km}^3$ for Cariaco or $32,398 \text{ km}^3$ for the Black Sea). We can assess some

597 aspects of the response of Orca Basin to the placement and remineralization of organic matter, but the
598 extreme ionic strength of Orca Basin exceeds the range of known equilibrium constants for the carbonate
599 system and prevents meaningful pH calculations. We also lack sufficient understanding of the unusual
600 Orca Basin microbial community (Nigro et al., 2020) to constrain the relative importance of
601 methanogenesis and MSR within the brine. For illustration purposes, however, we can assume that some
602 fraction of sequestered biomass breaks down through MSR and/or methanogenesis at a rate that is at least
603 much faster than the rate of mixing across the water-brine interface.

604 Given the small volume of the brine, the *in situ* respiration of 0.05 Tmol C (2.2 Tg CO₂ equivalent) by
605 MSR alone would increase DIC concentrations from 4.7 mM to 9.6 mM and simultaneously increase
606 alkalinity from 4.4 mM to between 9.3 and 11.4 mM, depending on mean respired organic matter redox
607 state. This amount of MSR would generate 2.4–3.5 mM H₂S and would increase NH₄⁺ from 0.5 mM to
608 ~1.2 mM. Alternatively, if breakdown proceeded exclusively via (methylotrophic) methanogenesis,
609 breakdown of the same amount of organic carbon could increase DIC from 4.7 mM to 6.1–9.6 mM
610 without adding alkalinity, lowering brine pH. The resulting methane would be sufficient to approximately
611 double the already high natural concentrations of CH₄ in the brine (3.4 mM).

612 To place the results of this calculation in context, we need additional information about the rates of
613 organic matter degradation within the Orca Basin brine and the ability of its slow-growing community to
614 respond to a dramatic increase in carbon availability. The microbial community in Orca Basin consists
615 primarily of halophilic sulfate reducers, methanogens, and ammonium oxidizers (Nigro et al., 2020), and
616 rates of potential sulfate reduction are low and similar to other hypersaline brines (~10 to 76 nmol cm⁻³ d⁻¹;
617 Hurtgen et al., 1999; Zhuang et al., 2016). Despite low rates of MSR and methanogenesis, Orca Basin is
618 highly effective at minimizing breakdown of at least some types of organic matter. Well-preserved
619 seaweeds and their epibionts and lipids have been described from Orca Basin sediments below 10 m
620 depth, which is virtually unheard of in other settings (Kennett and Penrose, 1978; Harvey and Kennicutt,
621 1992) and indicates a remarkable absence or selectivity of heterotrophic degradation. Although electron
622 acceptors (e.g., sulfate) are plentiful, organic materials are also abundant within the brine: DOM
623 concentrations reach 0.24 mM DOC, and sinking particulate organic matter provides a consistent marine
624 C source (Trefry, 1984; Shah et al., 2013; Diercks et al., 2019).

625 Many unknowns therefore remain about the capacity of microbial communities in anoxic, hypersaline
626 basins to respond to rapid increases in organic carbon loading. Experiments are needed to assess the
627 relative importance of sulfate reduction versus methylotrophic methanogenesis for biomass breakdown in
628 hypersaline basins, and the sensitivity of breakdown rates to hypersaline conditions. Evidence for
629 stimulated methanogenesis could represent a risk for enhanced methane release to the overlying water

630 column, and although oxic methanotrophy in the Gulf of Mexico can be relatively efficient (Kessler et al.,
631 2011), the response of aerobic methane oxidizers in the water column requires further investigation.

632 Due to minimal mixing across the pycnocline, both solid- and dissolved-phase C in this system would be
633 physically sequestered over kyr timescales. The effects of stimulated MSR are likely limited to the brine
634 itself, although significant sulfide addition would make the brine sulfidic and impact metal cycling,
635 primarily Fe and Mn. In order to assess the release of breakdown products and background hydrocarbons
636 to the overlying water column in either endmember case, field data are needed related to how biomass
637 sinking impacts mixing at the Orca Basin pycnocline. The scale of potential mixing in a real deployment
638 would depend on the engineering choices that allow ballasted or densified biomass to sink through the
639 pycnocline.

640

641 **5. Summary and Conclusions: CDR potential of anoxic basins and key unknowns**

642 Any future attempts at effective and responsible CDR are futile in the absence of immediate and dramatic
643 CO₂ emissions reductions on a global scale and must be pursued in that context; emissions reductions are
644 the most cost-effective and highest net reduction strategy currently available (IPCC AR6, 2023). If marine
645 CDR is pursued as an approach to support decarbonization, its methods will need to both minimize
646 ecological risks and maximize storage durability. Risk minimization will also require effective
647 monitoring, reporting, and verification (MRV) to account for the actual efficiency of CO₂ storage in
648 various parts of the ocean system.

649 By these criteria, anoxic basins in general and the Black Sea in particular may represent uniquely
650 effective locations for the durable sequestration of atmospheric CO₂ as organic carbon. This process
651 conceptually accelerates a central mechanism for climate recovery in the natural Earth system. Anoxic
652 basins may reduce geochemical and ecological risks relative to well-oxygenated regions, where biomass
653 degradation will have larger impacts on pH change and deep-sea ecosystems. Careful consideration of
654 benthic impacts is crucial for any such activity (Levin et al., 2023).

655 The effective capacity of anoxic basins for CO₂ removal depends on the efficiency of organic carbon
656 storage, which depends in turn on the stoichiometry and reactivity of the biomass materials selected.
657 Although the Black Sea has by far the largest capacity for organic carbon sequestration, smaller but
658 complementary contributions may be achievable from Cariaco Basin and anoxic hypersaline basins like
659 Orca Basin. A primary challenge for CDR applications in Cariaco Basin will be the high and variable
660 rates of upwelling in the basin, which will ventilate remineralized CO₂. For Orca Basin, a primary
661 challenge is predicting biogeochemical behavior at very high ionic strength, necessitating site-specific

662 studies of the relative favorability of microbial breakdown processes. In all of these cases, the
663 morphology and circulation of anoxic marine basins present opportunities for effective monitoring,
664 reporting and verification of CO₂ sequestration and environmental effects. The combination of pH, DIC,
665 and alkalinity data can constrain the relative rates of organic matter remineralization via microbial sulfate
666 reduction and methanogenesis.

667 Additional research is needed to fill several key gaps in our ability to predict carbon cycling impacts of
668 organic matter addition to anoxic basins and to inform decision making related to its potential future
669 implementation as a CDR strategy. At a minimum, we will need to (1) test and parameterize
670 remineralization rates for specific types and components of biomass under relevant conditions; (2)
671 investigate the scale and recalcitrance of DOM generated from sequestered biomass; (3) evaluate the
672 impacts of biomass placement on benthic carbon turnover and chemical profiles in sediments, and (4)
673 develop basin-specific models for the physical transport and mixing effects of potential operations. These
674 remaining scientific challenges are substantial, but anoxic marine basins have the potential to be
675 substantive contributors to a global portfolio of CO₂ removal technologies and should be a priority for
676 additional focused investigation.

677

678

679 **Acknowledgments and Disclosures**

680 We thank Adam Subhas (WHOI) and Max Lloyd (Penn State) for valuable discussions about carbonate
681 chemistry and lignin breakdown pathways. We also thank Cameron Allen (UCSB) for his assistance with
682 the early stages of the project.

683 Funding for this work was provided by a grant to UCSB from the Grantham Foundation for the Protection
684 of the Environment.

685 In addition to her primary role as UCSB faculty, Raven serves as the Chief Science Officer for, and holds
686 minor (<3%) equity in, Carboniferous, Inc., a seed-funded startup company exploring potential
687 applications of deep marine biomass sequestration. The research presented here was conducted and
688 funded entirely via research grants to UCSB. An unconflicted PI is formally involved for all CDR-related
689 funds and mentorship plans in the Raven group.

690

691

692



698 Addy S. K. and Behrens E. W. (1980) Time of accumulation of hypersaline anoxic brine in Orca basin (Gulf of Mexico). *Marine*
699 *Geology* **37**, 241–252.

700 Agarwal A., Rana M. and Park J.-H. (2018) Advancement in technologies for the depolymerization of lignin. *Fuel Processing*
701 *Technology* **181**, 115–132.

702 Aguilar I., Sabatier P., Beck C., Audemard F., Crouzet C., Urbani F. and Campos C. (2017) Calculation of the reservoir age from
703 organic and carbonate fractions of sediments in the Gulf of Cariaco (Caribbean Sea). *Quaternary Geochronology* **38**,
704 50–60.

705 Aller R. C. (1994) Bioturbation and remineralization of sedimentary organic matter: effects of redox oscillation. *Chemical*
706 *Geology*, 15.

707 Aller R. C. and Cochran J. K. (2019) The Critical Role of Bioturbation for Particle Dynamics, Priming Potential, and Organic C
708 Remineralization in Marine Sediments: Local and Basin Scales. *Front. Earth Sci.* **7**, 157.

709 Anderson L. A. and Sarmiento J. L. (1994) Redfield ratios of remineralization determined by nutrient data analysis. *Global*
710 *Biogeochem. Cycles* **8**, 65–80.

711 Armstrong McKay D. I., Staal A., Abrams J. F., Winkelmann R., Sakschewski B., Loriani S., Fetzer I., Cornell S. E., Rockström
712 J. and Lenton T. M. (2022) Exceeding 1.5°C global warming could trigger multiple climate tipping points. *Science* **377**,
713 eabn7950.

714 Ballard R. D., Hiebert F. T., Coleman D. F., Ward C., Smith J. S., Willis K., Foley B., Croff K., Major C. and Torre F. (2001)
715 Deepwater Archaeology of the Black Sea: The 2000 Season at Sinop, Turkey. *American Journal of Archaeology* **105**,
716 607–623.

717 Benner R., Maccubbin A. E. and Hodson R. E. (1984) Anaerobic Biodegradation of the Lignin and Polysaccharide Components
718 of Lignocellulose and Synthetic Lignin by Sediment Microflora. *Appl Environ Microbiol* **47**, 998–1004.

719 Benner R., Moran M. A. and Hodson R. E. (1986) Biogeochemical cycling of lignocellulosic carbon in marine and freshwater
720 ecosystems: Relative contributions of procaryotes and eucaryotes: Aquatic lignocellulose degradation. *Limnol.*
721 *Oceanogr.* **31**, 89–100.

722 Bianchi T. S., Cui X., Blair N. E., Burdige D. J., Eglinton T. I. and Galy V. (2018) Centers of organic carbon burial and oxidation
723 at the land-ocean interface. *Organic Geochemistry* **115**, 138–155.

724 Boyd P. W., Bach L. T., Hurd C. L., Paine E., Raven J. A. and Tamsitt V. (2022) Potential negative effects of ocean afforestation
725 on offshore ecosystems. *Nat Ecol Evol* **6**, 675–683.

726 Boye K., Noël V., Tfaily M. M., Bone S. E., Williams K. H., Bargar J. R. and Fendorf S. (2017) Thermodynamically controlled
727 preservation of organic carbon in floodplains. *Nature Geosci* **10**, 415–419.

728 Committee on A Research Strategy for Ocean-based Carbon Dioxide Removal and Sequestration, Ocean Studies Board, Division
729 on Earth and Life Studies, and National Academies of Sciences, Engineering, and Medicine (2022) *A Research*
730 *Strategy for Ocean-based Carbon Dioxide Removal and Sequestration.*, National Academies Press, Washington, D.C.

731 Cowie G. L. and Hedges J. I. (1992) Sources and reactivities of amino acids in a coastal marine environment. *Limnol. Oceanogr.*
732 **37**, 703–724.

733 Diercks A., Ziervogel K., Sibert R., Joye S. B., Asper V. and Montoya J. P. (2019) Vertical marine snow distribution in the
734 stratified, hypersaline, and anoxic Orca Basin (Gulf of Mexico) eds. J. W. Deming and L. Thomsen. *Elementa: Science*
735 *of the Anthropocene* **7**, 10.

736 van Dongen B. E., Schouten S. and Sinninghe Damsté J. S. (2006) Preservation of carbohydrates through sulfurization in a
737 Jurassic euxinic shelf sea: Examination of the Blackstone Band TOC cycle in the Kimmeridge Clay Formation, UK.
738 *Organic Geochemistry* **37**, 1052–1073.

739 Du Vivier A. D. C., Jacobson A. D., Lehn G. O., Selby D., Hurtgen M. T. and Sageman B. B. (2015) Ca isotope stratigraphy
740 across the Cenomanian–Turonian OAE 2: Links between volcanism, seawater geochemistry, and the carbonate
741 fractionation factor. *Earth and Planetary Science Letters* **416**, 121–131.

742 Dubinin A. V., Demidova T. P., Dubinina E. O., Rimskaya-Korsakova M. N., Semilova L. S., Berezhnaya E. D., Klyuvitkin A.
743 A., Kravchishina M. D. and Belyaev N. A. (2022) Sinking particles in the Black Sea waters: Vertical fluxes of elements
744 and pyrite to the bottom, isotopic composition of pyrite sulfur, and hydrogen sulfide production. *Chemical Geology*
745 **606**, 120996.

746 Egorov V. N., Artemov Y. G., Gulín S. B. and Polikarpov G. (2011) Methane seeps in the Black Sea: discovery, quantification
747 and environmental assessment. , 15.

748 Fanning K. A. and Pilson M. E. Q. (1972) A model for the anoxic zone of the Cariaco Trench. *Deep Sea Research and*
749 *Oceanographic Abstracts* **19**, 847–863.

750 Fenchel T. (2012) Protozoa and oxygen. *Acta protozoologica* **52**, 11.

751 Fraser C. I., Nikula R. and Waters J. M. (2011) Oceanic rafting by a coastal community. *Proc. R. Soc. B.* **278**, 649–655.

- 752 Froelich P. N., Klinkhammer G. P., Bender M. L., Luedtke N. A., Heath G. R., Cullen D., Dauphin P. and Blaynehartman D.
753 Hammond. (1979) Early oxidation of organic matter in pelagic sediments of the eastern equatorial Atlantic: suboxic
754 diagenesis. *Geochimica et Cosmochimica Acta* **43**, 1075–1090.
- 755 Gallagher K. L., Kading T. J., Braissant O., Dupraz C. and Visscher P. T. (2012) Inside the alkalinity engine: the role of electron
756 donors in the organomineralization potential of sulfate-reducing bacteria. *Geobiology* **10**, 518–530.
- 757 Hartnett H. E., Keil R. G., Hedges J. I. and Devol A. H. (1998) Influence of oxygen exposure time on organic carbon
758 preservation in continental margin sediments. *Nature* **391**, 572–575.
- 759 Harvey H. R. and Kennicutt M. C. (1992) Selective alteration of Sargassum lipids in anoxic sediments of the Orca Basin.
760 *Organic Geochemistry* **18**, 181–187.
- 761 Hastings D. and Emerson S. (1988) Sulfate reduction in the presence of low oxygen levels in the water column of the Cariaco
762 Trench: Oxidic sulfate reduction. *Limnol. Oceanogr.* **33**, 391–396.
- 763 Hedges J. I. and Keil R. G. (1995) Sedimentary organic matter preservation: an assessment and speculative synthesis. *Marine
764 Chemistry* **49**, 81–115.
- 765 Hess M., Paul S. S., Puniya A. K., van der Giezen M., Shaw C., Edwards J. E. and Fliegerová K. (2020) Anaerobic Fungi: Past,
766 Present, and Future. *Front. Microbiol.* **11**, 584893.
- 767 Hiscock W. T. and Millero F. J. (2006) Alkalinity of the anoxic waters in the Western Black Sea. *Deep Sea Research Part II:
768 Topical Studies in Oceanography* **53**, 1787–1801.
- 769 Hülse D., Arndt S. and Ridgwell A. (2019) Mitigation of Extreme Ocean Anoxic Event Conditions by Organic Matter
770 Sulfurization. *Paleoceanography and Paleoclimatology* **34**, 476–489.
- 771 Hülse D., Lau K. V., van de Velde S. J., Arndt S., Meyer K. M. and Ridgwell A. (2021) End-Permian marine extinction due to
772 temperature-driven nutrient recycling and euxinia. *Nat. Geosci.* **14**, 862–867.
- 773 Hulthe G., Hulth S. and Hall P. O. J. (1998) Effect of oxygen on degradation rate of refractory and labile organic matter in
774 continental margin sediments. *Geochimica et Cosmochimica Acta* **62**, 1319–1328.
- 775 Hurtgen M. T., Lyons T., Ingall E. and Cruse A. (1999) Anomalous enrichments of iron monosulfide in euxinic marine sediments
776 and the role of H₂S in iron sulfide transformations; examples from Effingham Inlet, Orca Basin, and the Black Sea.
777 *American Journal of Science* **299**, 556–588.
- 778 IPCC, 2022: Climate Change 2022: Impacts, Adaptation, and Vulnerability. Contribution of Working Group II to the Sixth
779 Assessment Report of the Intergovernmental Panel on Climate Change [H.-O. Pörtner, D.C. Roberts, M. Tignor, E.S.
780 Poloczanska, K. Mintenbeck, A. Alegria, M. Craig, S. Langsdorf, S. Löschke, V. Möller, A. Okem, B. Rama (eds.)].
781 Cambridge University Press. Cambridge University Press, Cambridge, UK and New York, NY, USA, 3056 pp.,
782 doi:10.1017/9781009325844.
- 783 Ivanov L. I. and Samodurov A. S. (2001) The role of lateral fluxes in ventilation of the Black Sea. *Journal of Marine Systems* **31**,
784 159–174.
- 785 Jarvis I., Lignum J. S., Gröcke D. R., Jenkyns H. C. and Pearce M. A. (2011) Black shale deposition, atmospheric CO₂
786 drawdown, and cooling during the Cenomanian-Turonian Oceanic Anoxic Event: CO₂ drawdown and cooling during
787 OAE2. *Paleoceanography* **26**, n/a-n/a.
- 788 Jørgensen B. B., Weber A. and Zopf J. (2001) Sulfate reduction and anaerobic methane oxidation in Black Sea sediments. *Deep
789 Sea Research Part I: Oceanographic Research Papers* **48**, 2097–2120.
- 790 Keil R. G., Nuwer J. M. and Strand S. E. (2010) Burial of agricultural byproducts in the deep sea as a form of carbon
791 sequestration: A preliminary experiment. *Marine Chemistry* **122**, 91–95.
- 792 Kennett J. P. and Penrose N. L. (1978) Fossil Holocene seaweed and attached calcareous polychaetes in an anoxic basin, Gulf of
793 Mexico. *Nature* **276**, 172–173.
- 794 Kessler J. D., Valentine D. L., Redmond M. C., Du M., Chan E. W., Mendes S. D., Quiroz E. W., Villanueva C. J., Shusta S. S.,
795 Werra L. M., Yvon-Lewis S. A. and Weber T. C. (2011) A Persistent Oxygen Anomaly Reveals the Fate of Spilled
796 Methane in the Deep Gulf of Mexico. *Science* **331**, 312–315.
- 797 Kohnen M. E. L., Damsté J. S. S., Kock-van Dalen A. C., Haven H. L. T., Rullkötter J. and De Leeuw J. W. (1990) Origin and
798 diagenetic transformations of C₂₅ and C₃₀ highly branched isoprenoid sulphur compounds: Further evidence for the
799 formation of organically bound sulphur during early diagenesis. *Geochimica et Cosmochimica Acta* **54**, 3053–3063.
- 800 Konovalov S. K. and Murray J. W. (2001) Variations in the chemistry of the Black Sea on a time scale of decades (1960–1995).
801 *Journal of Marine Systems* **31**, 217–243.
- 802 Krause-Jensen D. and Duarte C. M. (2016) Substantial role of macroalgae in marine carbon sequestration. *Nature Geosci* **9**, 737–
803 742.
- 804 Kristjansson J. K., Schønheit P. and Thauer R. K. (1982) Different K_s values for hydrogen of methanogenic bacteria and sulfate
805 reducing bacteria: An explanation for the apparent inhibition of methanogenesis by sulfate. *Arch. Microbiol.* **131**, 278–
806 282.
- 807 Kuhnt W., Holbourn A. E., Beil S., Aquit M., Krawczyk T., Flögel S., Chellai E. H. and Jabour H. (2017) Unraveling the onset of
808 Cretaceous Oceanic Anoxic Event 2 in an extended sediment archive from the Tarfaya-Laayoune Basin, Morocco:
809 Tarfaya OAE2 Onset. *Paleoceanography* **32**, 923–946.
- 810 LaRock P. A., Lauer R. D., Schwarz J. R., Watanabe K. K. and Wiesenburg D. A. (1979) Microbial Biomass and Activity
811 Distribution in an Anoxic, Hypersaline Basin. *Appl Environ Microbiol* **37**, 466–470.
- 812 Lee B.-S., Bullister J. L., Murray J. W. and Sonnerup R. E. (2002) Anthropogenic chlorofluorocarbons in the Black Sea and the
813 Sea of Marmara. *Deep Sea Research Part I: Oceanographic Research Papers* **49**, 895–913.

814 Lee C. (1992) Controls on organic carbon preservation: The use of stratified water bodies to compare intrinsic rates of
815 decomposition in oxic and anoxic systems. *Geochimica et Cosmochimica Acta* **56**, 3323–3335.

816 Levin L. A., Alfaro-Lucas J. M., Colaço A., Cordes E. E., Craik N., Danovaro R., Hoving H.-J., Ingels J., Mestre N. C., Seabrook
817 S., Thurber A. R., Vivian C. and Yasuhara M. (2023) Deep-sea impacts of climate interventions. *Science* **379**, 978–981.

818 Li M., Pu Y. and Ragauskas A. J. (2016) Current Understanding of the Correlation of Lignin Structure with Biomass
819 Recalcitrance. *Front. Chem.* **4**.

820 Lyons W. B., Long D. T., Hines M. E., Gaudette H. E. and Armstrong P. B. (1984) Calcification of cyanobacterial mats in Solar
821 Lake, Sinai. *Geol* **12**, 623.

822 Marchand C., Disnar J. R., Lallier-Vergès E. and Lottier N. (2005) Early diagenesis of carbohydrates and lignin in mangrove
823 sediments subject to variable redox conditions (French Guiana). *Geochimica et Cosmochimica Acta* **69**, 131–142.

824 Markova N. V. (2023) The Black Sea Deep-Water Circulation: Recent Findings and Prospects for Research. In *Processes in*
825 *GeoMedia—Volume VI* (ed. T. Chaplina). Springer Geology. Springer International Publishing, Cham. pp. 553–564.

826 Mayumi D., Mochimaru H., Tamaki H., Yamamoto K., Yoshioka H., Suzuki Y., Kamagata Y. and Sakata S. (2016) Methane
827 production from coal by a single methanogen. *Science* **354**, 222–225.

828 Middelburg J. J., Soetaert K. and Hagens M. (2020) Ocean Alkalinity, Buffering and Biogeochemical Processes. *Rev. Geophys.*
829 **58**.

830 Muller-Karger F. E., Astor Y. M., Benitez-Nelson C. R., Buck K. N., Fanning K. A., Lorenzoni L., Montes E., Rueda-Roa D. T.,
831 Scranton M. I., Tappa E., Taylor G. T., Thunell R. C., Troccoli L. and Varela R. (2019) The Scientific Legacy of the
832 CARIACO Ocean Time-Series Program. *Annu. Rev. Mar. Sci.* **11**, 413–437.

833 Muller-Karger F., Varela R., Thunell R., Astor Y., Zhang H., Luerssen R. and Hu C. (2004) Processes of coastal upwelling and
834 carbon flux in the Cariaco Basin. *Deep Sea Research Part II: Topical Studies in Oceanography* **51**, 927–943.

835 Murray J. W., Top Z. and Özsoy E. (1991) Hydrographic properties and ventilation of the Black Sea. *Deep Sea Research Part A.*
836 *Oceanographic Research Papers* **38**, S663–S689.

837 Nauhaus K., Albrecht M., Elvert M., Boetius A. and Widdel F. (2007) In vitro cell growth of marine archaeal-bacterial consortia
838 during anaerobic oxidation of methane with sulfate. *Environ Microbiol* **9**, 187–196.

839 Nigro L. M., Elling F. J., Hinrichs K.-U., Joye S. B. and Teske A. (2020) Microbial ecology and biogeochemistry of hypersaline
840 sediments in Orca Basin ed. W. J. Brazelton. *PLoS ONE* **15**, e0231676.

841 Ocean Visions and Monterey Bay Aquarium Research Institute, “Answering Critical Questions About Sinking Macroalgae for
842 Carbon Dioxide Removal: A Research Framework to Investigate Sequestration Efficacy and Environmental Impacts,”
843 2022.

844 Orcutt B. N., Bradley J. A., Brazelton W. J., Estes E. R., Goordial J. M., Huber J. A., Jones R. M., Mahmoudi N., Marlow J. J.,
845 Murdock S. and Pachiadaki M. (2020) Impacts of deep-sea mining on microbial ecosystem services. *Limnol Oceanogr*
846 **65**, 1489–1510.

847 Oremland R. S. and Polcin S. (1982) Methanogenesis and Sulfate Reduction: Competitive and Noncompetitive Substrates in
848 Estuarine Sediments. *Applied and Environmental Microbiology* **44**.

849 Östlund H. G. (1974) Expedition "Odysseus 65" . Radiocarbon age of Black Sea Water. In: The Black Sea: Geology, chemistry
850 and biology , E . T . Degens and D . A . Ross, editors, American Association of Petroleum Geologists , Memoir 20, pp.
851 127-132.

852 Owens J. D., Lyons T. W. and Lowery C. M. (2018) Quantifying the missing sink for global organic carbon burial during a
853 Cretaceous oceanic anoxic event. *Earth and Planetary Science Letters* **499**, 83–94.

854 Owens J. D., Reinhard C. T., Rohrsen M., Love G. D. and Lyons T. W. (2016) Empirical links between trace metal cycling and
855 marine microbial ecology during a large perturbation to Earth’s carbon cycle. *Earth and Planetary Science Letters* **449**,
856 407–417.

857 Paine E. R., Schmid M., Boyd P. W., Diaz-Pulido G. and Hurd C. L. (2021) Rate and fate of dissolved organic carbon release by
858 seaweeds: A missing link in the coastal ocean carbon cycle ed. C. Pfister. *J. Phycol.* **57**, 1375–1391.

859 Porter D., Roychoudhury A. N. and Cowan D. (2007) Dissimilatory sulfate reduction in hypersaline coastal pans: Activity across
860 a salinity gradient. *Geochimica et Cosmochimica Acta* **71**, 5102–5116.

861 Raven M. R., Fike D. A., Bradley A. S., Gomes M. L., Owens J. D. and Webb S. A. (2019) Paired organic matter and pyrite $\delta^{34}\text{S}$
862 records reveal mechanisms of carbon, sulfur, and iron cycle disruption during Ocean Anoxic Event 2. *Earth and*
863 *Planetary Science Letters* **512**, 27–38.

864 Raven M. R., Fike D. A., Gomes M. L., Webb S. M., Bradley A. S. and McClelland H.-L. O. (2018) Organic carbon burial
865 during OAE2 driven by changes in the locus of organic matter sulfurization. *Nat Commun* **9**, 3409.

866 Raven M. R., Keil R. G. and Webb S. M. (2021) Rapid, Concurrent Formation of Organic Sulfur and Iron Sulfides During
867 Experimental Sulfurization of Sinking Marine Particles. *Global Biogeochem Cycles* **35**.

868 Raven M. R., Sessions A. L., Adkins J. F. and Thunell R. C. (2016) Rapid organic matter sulfurization in sinking particles from
869 the Cariaco Basin water column. *Geochimica et Cosmochimica Acta* **190**, 175–190.

870 Redfield A. C. (1934) On the Proportions of Organic Derivatives in Sea Water and Their Relation to the Composition of
871 Plankton.

872 Reeburgh W. S. (1976) Methane consumption in Cariaco Trench waters and sediments. *Earth and Planetary Science Letters* **28**,
873 337–344.

874 Reeburgh W. S., Ward B. B., Whalen S. C., Sandbeck K. A., Kilpatrick K. A. and Kerkhof L. J. (1991) Black Sea methane
875 geochemistry. *Deep Sea Research Part A. Oceanographic Research Papers* **38**, S1189–S1210.

- 876 Ryan W. B. F., Pitman W. C., Major C. O., Shimkus K., Moskalenko V., Jones G. A., Dimitrov P., Gorür N., Sakinç M. and
877 Yüce H. (1997) An abrupt drowning of the Black Sea shelf. *Marine Geology* **138**, 119–126.
- 878 Schlanger S. O. and Jenkyns H. C. (1976) Cretaceous Oceanic Anoxic Events: Causes and consequences. *GEOLOGIE EN*
879 *MIJNBOUW* **55**, 179–184.
- 880 Schmale O., Greinert J. and Rehder G. (2005) Methane emission from high-intensity marine gas seeps in the Black Sea into the
881 atmosphere: Methane emission from marine gas seeps. *Geophys. Res. Lett.* **32**, n/a-n/a.
- 882 Schmale O., Haeckel M. and McGinnis D. F. (2011) Response of the Black Sea methane budget to massive short-term submarine
883 inputs of methane. *Biogeosciences* **8**, 911–918.
- 884 Scranton M. I. (1988) Temporal variations in the methane content of the Cariaco Trench. *Deep Sea Research Part A.*
885 *Oceanographic Research Papers* **35**, 1511–1523.
- 886 Scranton M. I., Astor Y., Bohrer R., Ho T.-Y. and Muller-Karger F. (2001) Controls on temporal variability of the geochemistry
887 of the deep Cariaco Basin. *Deep Sea Research Part I: Oceanographic Research Papers* **48**, 1605–1625.
- 888 Scranton M. I., Sayles F. L., Bacon M. P. and Brewer P. G. (1987) Temporal changes in the hydrography and chemistry of the
889 Cariaco Trench. *Deep Sea Research Part A. Oceanographic Research Papers* **34**, 945–963.
- 890 Sexton P. F., Norris R. D., Wilson P. A., Pälke H., Westerhold T., Röhl U., Bolton C. T. and Gibbs S. (2011) Eocene global
891 warming events driven by ventilation of oceanic dissolved organic carbon. *Nature* **471**, 349–352.
- 892 Shah S. R., Joye S. B., Brandes J. A. and McNichol A. P. (2013) Carbon isotopic evidence for microbial control of carbon supply
893 to Orca Basin at the seawater–brine interface. *Biogeosciences* **10**, 3175–3183.
- 894 Sheu D.-D. and Presley B. J. (1986) Variations of calcium carbonate, organic carbon and iron sulfides in anoxic sediment from
895 the Orca Basin, Gulf of Mexico. *Marine Geology* **70**, 103–118.
- 896 Shokes R. F., Trabant P. K., Presley B. J. and Reid D. F. (1977) Anoxic, Hypersaline Basin in the Northern Gulf of Mexico.
897 *Science* **196**, 1443–1446.
- 898 Siegel D. A., DeVries T., Doney S. C. and Bell T. (2021) Assessing the sequestration time scales of some ocean-based carbon
899 dioxide reduction strategies. *Environ. Res. Lett.* **16**, 104003.
- 900 Sinninghe Damsté J. S. and Köster J. (1998) A euxinic southern North Atlantic Ocean during the Cenomanian/Turonian oceanic
901 anoxic event. *Earth and Planetary Science Letters* **158**, 165–173.
- 902 Sinsabaugh R. L. (2010) Phenol oxidase, peroxidase and organic matter dynamics of soil. *Soil Biology and Biochemistry* **42**,
903 391–404.
- 904 Stanev E. V., Chtirkova B. and Peneva E. (2021) Geothermal Convection and Double Diffusion Based on Profiling Floats in the
905 Black Sea. *Geophysical Research Letters* **48**.
- 906 Starostenko V. I., Rusakov O. M., Shnyukov E. F., Kobolev V. P. and Kutas R. I. (2010) Methane in the northern Black Sea:
907 characterization of its geomorphological and geological environments. *SP* **340**, 57–75.
- 908 Stewart K., Kassakian S., Krynytzky M., DiJulio D. and Murray J. W. (2007) Oxidic, suboxic, and anoxic conditions in the Black
909 Sea. In *The Black Sea Flood Question: Changes in Coastline, Climate, and Human Settlement* (eds. V. Yanko-
910 Hombach, A. S. Gilbert, N. Panin, and P. M. Dolukhanov). Springer Netherlands. pp. 1–21.
- 911 Trefry J. H. (1984) Distribution and chemistry of manganese, iron, and suspended particulates in Orca Basin. *Geo-Marine Letter*
912 **4**, 125–130.
- 913 Tribovillard N., Bout-Roumazeilles V., Algeo T., Lyons T. W., Sionneau T., Montero-Serrano J. C., Riboulleau A. and Baudin F.
914 (2008) Paleodepositional conditions in the Orca Basin as inferred from organic matter and trace metal contents. *Marine*
915 *Geology* **254**, 62–72.
- 916 Valentine D. L. (2011) Emerging Topics in Marine Methane Biogeochemistry. *Annu. Rev. Mar. Sci.* **3**, 147–171.
- 917 Van Cappellen P., Viollier E., Roychoudhury A., Clark L., Ingall E., Lowe K. and Dichristina T. (1998) Biogeochemical Cycles
918 of Manganese and Iron at the Oxidic–Anoxic Transition of a Stratified Marine Basin (Orca Basin, Gulf of Mexico).
919 *Environ. Sci. Technol.* **32**, 2931–2939.
- 920 Wakeham S. G., Lewis C. M., Hopmans E. C., Schouten S. and Sinninghe Damsté J. S. (2003) Archaea mediate anaerobic
921 oxidation of methane in deep euxinic waters of the Black Sea. *Geochimica et Cosmochimica Acta* **67**, 1359–1374.
- 922 Ward B. B., Kilpatrick K. A., Novelli P. C. and Scranton M. I. (1987) Methane oxidation and methane fluxes in the ocean surface
923 layer and deep anoxic waters. *Nature* **327**, 226–229.
- 924 Wiesenburg D. A., Brooks J. M. and Bernard B. B. (1985) Biogenic hydrocarbon gases and sulfate reduction in the Orca Basin
925 brine. *Geochimica et Cosmochimica Acta* **49**, 2069–2080.
- 926 Young L. Y. and Frazer A. C. (1987) The fate of lignin and lignin-derived compounds in anaerobic environments.
927 *Geomicrobiology Journal* **5**, 261–293.
- 928 Zhang J.-Z. and Millero F. J. (1993) The chemistry of the anoxic waters in the Cariaco Trench. *Deep Sea Research Part I:*
929 *Oceanographic Research Papers* **40**, 1023–1041.
- 930 Zhuang G.-C., Elling F. J., Nigro L. M., Samarkin V., Joye S. B., Teske A. and Hinrichs K.-U. (2016) Multiple evidence for
931 methylotrophic methanogenesis as the dominant methanogenic pathway in hypersaline sediments from the Orca Basin,
932 Gulf of Mexico. *Geochimica et Cosmochimica Acta* **187**, 1–20.
- 933 Zolotarev V. G., Sochel'nikov, V V and Malovitskiy, Ya P (1979) Heat flow in the Black and Mediterranean seas. *Oceanology*
934 **19**, 701–704.

935

936



937